Geological Society of America Special Papers Online First

Effects of Deccan volcanism on paleoenvironment and planktic foraminifera: A global survey

Jahnavi Punekar, Paula Mateo and Gerta Keller

E-mail alerting services	click www.gsapubs.org/cgi/alerts to receive free e-mail alerts when new articles cite this article
Subscribe	click www.gsapubs.org/subscriptions to subscribe to Geological Society of America Special Papers
Permission request	click www.geosociety.org/pubs/copyrt.htm#gsa to contact GSA.

Notes

THE
GEOLOGICAL
SOCIETY
OF AMERICA

Effects of Deccan volcanism on paleoenvironment and planktic foraminifera: A global survey

Jahnavi Punekar*
Paula Mateo
Gerta Keller
Department of Geosciences, Princeton University, Princeton, New Jersey 08544, USA

ABSTRACT

Deccan volcanism, one of Earth's largest flood basalt provinces, erupted ~80% of its total volume (phase 2) during a relatively short time in the uppermost Maastrichtian paleomagnetic chron C29r and ended with the Cretaceous-Tertiary boundary mass extinction. Full biotic recovery in the marine realm was delayed at least 500 k.y. or until after the last Deccan eruptions in C29n (phase 3, 14% of the total Deccan volume). For over 30 yr, the mass extinction has been commonly attributed to the Chicxulub impact, and the delayed recovery remained an enigma. Here, we demonstrate that the two phases of Deccan volcanism can account for both the mass extinction and delayed marine recovery.

In India, a direct correlation between Deccan eruptions (phase 2) and the mass extinction reveals that ~50% of the planktic foraminifer species gradually disappeared during volcanic eruptions prior to the first of four lava megaflows, reaching ~1500 km across India, and out to the Bay of Bengal. Another 50% disappeared after the first megaflow, and the mass extinction was complete with the last megaflow. Throughout this interval, blooms of the disaster opportunist *Guembelitria cretacea* dominate shallow-marine assemblages in coeval intervals from India to the Tethys and the Atlantic Oceans to Texas. Similar high-stress environments dominated by blooms of *Guembelitria* and/or *Globoconusa* are observed correlative with Deccan volcanism phase 3 in the early Danian C29n, followed by full biotic recovery after volcanism ended. The mass extinction and high-stress conditions may be explained by the intense Deccan volcanism leading to rapid global warming and cooling in C29r and C29n, enhanced weathering, continental runoff, and ocean acidification, resulting in a carbonate crisis in the marine environment.

*jpunekar@princeton.edu

INTRODUCTION

For over three decades, a large extraterrestrial impact has been advocated as the sole cause for the Cretaceous-Tertiary (K-T) boundary mass extinction (also known as the Cretaceous-Paleogene [or K-Pg] mass extinction), and Deccan volcanism in India was dismissed as ineffectual (see Schulte et al., 2010). In this scenario, the late Maastrichtian planktic foraminiferal turnover and survivorship across the mass extinction, first noted by Keller (1988a; Keller et al., 1995) were attributed to artifacts of the sedimentary record. A blind test was devised to prove that the mass extinction was a sudden event and left no survivors but one species, consistent with the impact hypothesis (Smit, 1982). When the blind test did not confirm this assumption, this test was considered inconclusive (Ginsburg, 1997a, 1997b, 1997c; Lipps, 1997).

Over the past 15 yr, these contested extinction and survivorship patterns and associated environmental changes have been documented worldwide and increasingly linked to the late Maastrichtian global warming and Deccan volcanism (e.g., Li and Keller, 1998a, 1998b; Abramovich et al., 1998; Keller, 2001, 2008a, 2008b, 2011; Keller et al., 2009a; Abramovich and Keller, 2003; Tobin et al., 2012). However, the proposed link remained speculative and vague, referring to Deccan volcanism as a single undifferentiated event largely expressed by the latest Maastrichtian global warming. Only with the documentation of Deccan volcanism as three distinct phases (Chenet et al., 2007, 2008, 2009) and the discovery and documentation of the direct link between the mass extinction and Deccan volcanism (Keller et al., 2008, 2009, 2011a, 2012) has it become possible to directly link environmental and faunal changes with specific phases of volcanism (see Keller, this volume).

The objective of this paper is to test the twin hypotheses:
(1) The main phase 2 of Deccan volcanism in C29r near the end of the Maastrichtian caused global high-stress conditions for planktic foraminifera that resulted in the mass extinction.
(2) Deccan phase 3 in the early Danian C29n prolonged environmental stress, preventing full marine recovery for about a half million years.

We evaluate these hypotheses based on previously published work and global archival data on planktic foraminifera and carbon and oxygen stable isotopes that may reveal the devastating environmental and climatic effects of these massive continental flood basalt eruptions. It is well known that Deccan phase 2 corresponds to the rapid global warming and cooling near the end of the Maastrichtian (Li and Keller, 1998b; Ravizza and Puecker-Ehrenbrink, 2003; MacLeod et al., 2005; Robinson et al., 2009) and more specifically in planktic foraminiferal zones CF2 and CF1, which span the last 120 k.y. and 160 k.y. of the late Maastrichtian paleomagnetic chron C29r, respectively (Li and Keller, 1998a, 1998b; Abramovich et al., 2002, 2003, 2011; Keller et al., 2011a, 2011b, 2012). Deccan phase 3 corresponds to the rapid global warming

in the early Danian known as the Dan-C2 event (Quillévéré et al., 2008; Coccioni et al., 2010) correlative with zone P1b of Keller et al. (1995, 2002a, 2011a, 2011b). Both climatic events are associated with major faunal changes, including blooms of the disaster opportunist *Guembelitria cretacea*, dwarfing of species, and decreased diversity in India and globally (Fig. 1). For this review, we choose localities that span from India through the Tethys and Atlantic Oceans to Texas, concentrating mainly on low to middle latitudes where the faunal effects were the most severe.

ENVIRONMENTAL EFFECTS OF VOLCANISM

Understanding the environmental and biological effects of large igneous province volcanism is nearly beyond comprehension. Recent studies are just beginning to provide a glimpse of the potentially devastating effects of sequential pulses of rapid, massive outpouring of lavas, and injection of ashes and gases (e.g., carbon dioxide, sulfur dioxide, chlorine, fluorine) during large igneous province emplacement (e.g., Columbia River, Deccan, Central Atlantic, and Siberian volcanic provinces; see Courtillot and Fluteau, this volume). For a basic understanding, we turn to a more recent example with fissure-type eruptions, such as Laki, Iceland, believed to be similar to Deccan volcanism.

Laki Eruptions of Iceland 1783–1784

From June 1783 to February 1784, Iceland was rocked by the largest volcanic eruption in human recorded history. About 130 craters opened along fissures in Earth's surface (Fig. 2A), and the rising magma interacted with groundwater, creating explosive lava fountains reaching heights of 900–1300 m. This volcanic eruption released an estimated 8 Megatons (Mt) of fluorine and ~122 Mt of sulfur dioxide (SO_2) into the atmosphere, ~0.91 km^3 of tephra (ash) blanketed Iceland and large parts of Europe, and 14.3 km^3 of basaltic lava spread over Iceland in 8 mo of volcanic activity (Thordarson and Self, 2003).

Convective currents of the eruption column carried ~20% of the sulfur mass released from the lava into the lower troposphere (~5 km), where it formed a local haze (Fig. 2B; Thordarson and Self, 2003). About 80% of the sulfur mass (~95 Mt of SO_2) released was carried to a height of 10–15 km into the upper troposphere–lower stratosphere, where sulfuric aerosols formed by reaction of SO_2 and atmospheric vapor produced ~200 Mt of H_2SO_4 aerosols that spread as distal haze across Europe (Thordarson and Self, 2003). About 175 Mt of the H_2SO_4 aerosols were removed as acid rain over Europe, causing extreme volcanic pollution and blanketing the region as dry fog (Stothers, 1996; Thordarson and Self, 2003), which resulted in severe climate extremes with dire consequences for humans and livestock. The excessive fluorine input resulted in fluorine poisoning, which along with the ensuing famine killed 20%–25% of the human population and 50%–80% of livestock on Iceland (Brayshay and Grattan, 1999; Grattan et al., 2003; Stone, 2004). Extreme summer heat in 1783 turned to extreme winter cold in 1784, and spring flooding
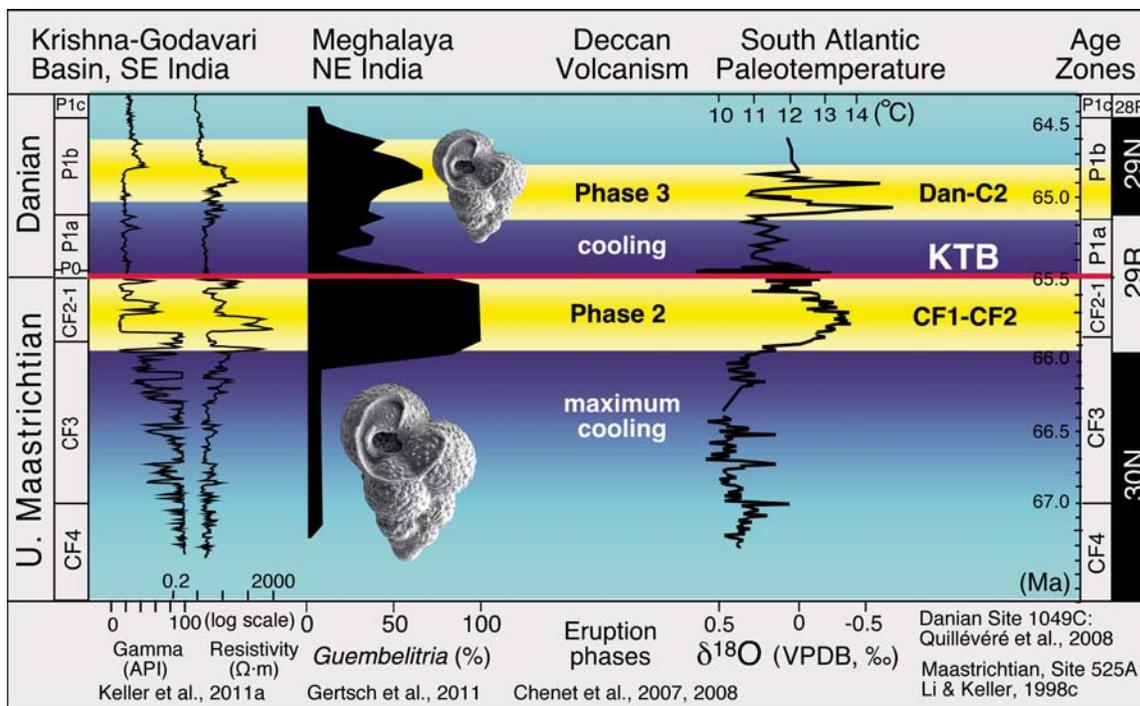
Effects of Deccan volcanism on paleoenvironment and planktic foraminifera: A global survey

Figure 1. *Guembelitria* blooms in northeastern and southeastern India correlate with Deccan volcanic phase 2 and phase 3 lava megaflows from deep wells in the Krishna-Godavari Basin. Deccan phase 2 and phase 3 volcanism is correlative with global warming events in the late Maastrichtian zones CF1–CF2 and the early Danian Dan-C2 event in zone P1b. KTB—Cretaceous-Tertiary boundary; API—American Petroleum Institute units; VPDB—Vienna Peedee belemnite.

caused tens of thousands of additional deaths across Europe and North America. A decade of extreme climate disruption followed, destroying crops and leading to famines.

Deccan Eruptions of India

Compared with the Deccan flood basalt eruptions, the Laki eruptions were inconsequential. During Deccan eruptions, an estimated 1.5 million km^3 of lava (100,000 times the size of Laki) flooded the continent; these deposits currently cover an area the size of France and were probably three times larger prior to erosion (Fig. 3; Raja Rao et al., 1999). This lava outpouring occurred in three phases, with the initial and smallest phase 1 (~6% of the total volume) in the early late Maastrichtian chron C30r/C30n ca. 67.4 Ma (or ca. 68.33 Ma according to *The Geologic Time Scale* of Gradstein et al., 2012). The second and largest phase 2 erupted ~80% of the total lava pile (~80,000 times the Laki eruptions) near the end of the Maastrichtian in chron C29r (Subbarao et al., 2000; Jay and Widdowson, 2008; Chenet et al., 2007, 2008), ending with the K-T boundary mass extinction (Keller et al., 2011a, 2012). The last phase 3 (~14% of the total volume) erupted in the early Danian chron C29n.

However, even more important factors than the size of lava eruptions were the tempo of emplacement and the amounts of SO_2, CO_2, Cl, and other gases released into the atmosphere. For the Deccan Traps, Chenet et al. (2007, 2009) estimated a total of 15,000–35,000 Gigatons (Gt) of CO_2 and 6500–17,000 Gt of SO_2 (compared with 0.122 Gt of SO_2 at Laki), with 80% erupting during phase 2. These totals do not account for the gases released by massive magma intrusions, contact metamorphism with limestones, coal deposits, and organic carbon–rich sediments, which could exceed the amount of magmatic gases (Ganino and Arndt, 2009; Courtillot and Fluteau, this volume; Mussard et al., this volume). The tempo of eruptions for each of the three main phases is difficult to estimate because each consisted of several single eruptive events with lava volumes of 1000 km^3 to 20,000 km^3 and some megaflows reaching ~1500 km across India and out into the Bay of Bengal. Emplacement of each single eruptive event is estimated at less than a decade, with each of the three phases emplaced over ~100 k.y., including times of no volcanic activity between flows (Chenet et al., 2009; Courtillot and Fluteau, this volume). This age estimate is consistent with biostratigraphic data for phase 2, which ends with the rapid emplacement of the four largest lava megaflows across India coincident with the K-T boundary mass extinction (Keller et al., 2011a, 2012). A similar sequence of megaflows ends Deccan Traps phase 3 in the early Danian.

Deccan Volcanism and Chicxulub Impact

How does the gas emission of Deccan volcanism compare with the Chicxulub impact? Chenet et al. (2008, 2009) estimated that the SO_2 and CO_2 flux of the Chicxulub impact may be
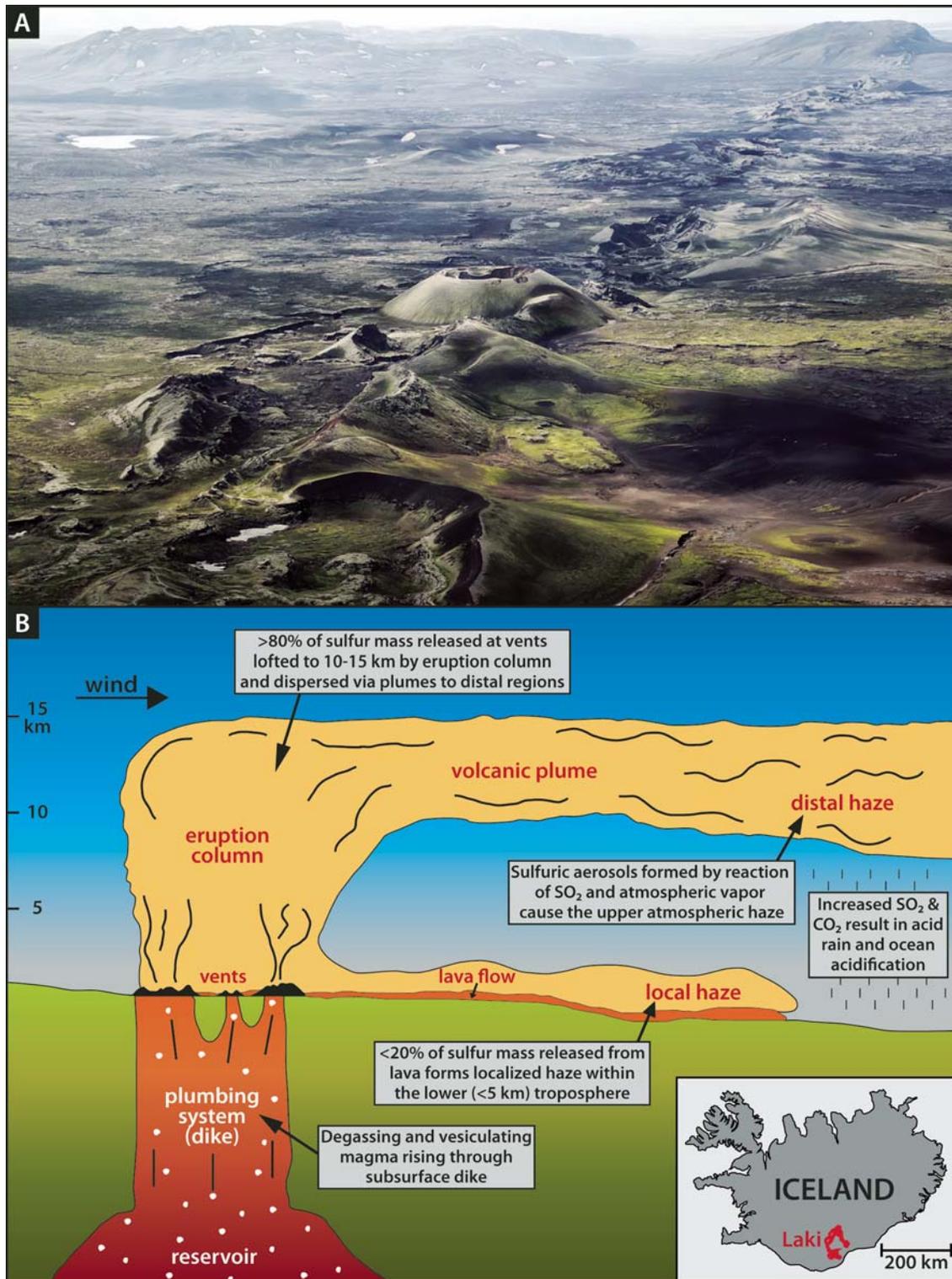
Figure 2. (A) Volcanoes dot the 1783–1784 Laki fissure eruptions of Iceland (photo by Klaus Ratzer, Germany, http://www.ratzer-art.de). (B) Schematic illustration of the Laki eruptions and distribution of volcanic gases (modified from Thordarson and Self, 2003). Similar fissure eruptions are believed to have characterized Deccan volcanism in India, although at a scale of ~100,000 times Laki today and ~300,000 times Laki prior to erosion.
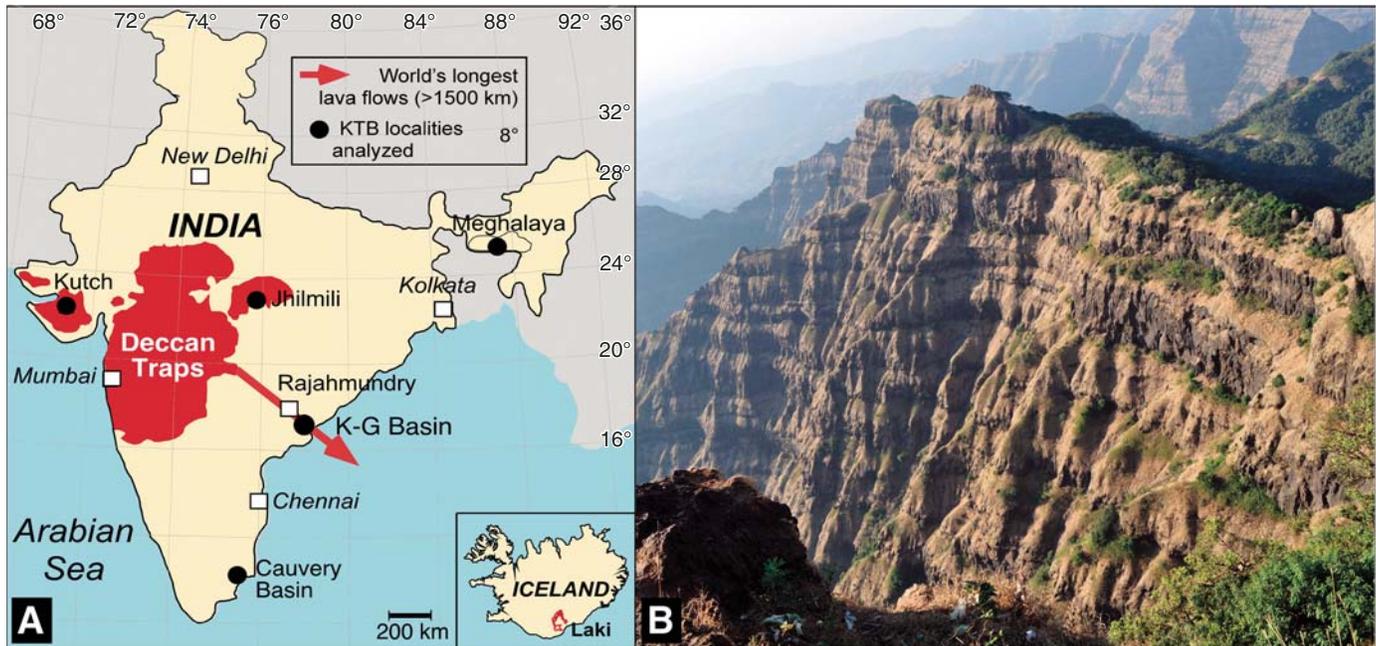
Figure 3. (A) Distribution of Deccan volcanic rocks in India today; prior to erosion, Deccan Trap basalts are believed to have covered about three times this area. Black circles mark sections studied. A map of Iceland with the area of the Laki eruptions is shown at the same relative size for comparison. (B) Photo shows the Deccan basalts forming 3000-m-high mountains near the Mahabaleshwar Hill Station in the Western Ghats. KTB—Cretaceous-Tertiary boundary; K-G—Krishna-Godavari Basin.

comparable to just one of the large single eruptive events of Deccan phase 2. However, the total Deccan gas output may have been on the order of 20–200 times that of the Chicxulub impact (Courtillot and Fluteau, this volume). Ultimately, the killing mechanism was not just the total gas output, but how rapidly eruptions followed each other. The environmental effects of a single event, such as the Chicxulub impact or one large Deccan eruption in phase 2, would have been relatively short-lived, and the environment would have recovered without necessarily causing species extinctions. Similarly, volcanic eruptions separated by long periods of quiet permit ecosystem recovery and the survival of most species. However, eruptions that follow each other in rapid succession prevent recovery and lead to runaway effects. This may have occurred at the end of the Maastrichtian, when lava eruptions followed in rapid succession with no evidence of long periods of inactivity, including the four lava megaflows that reached ~1500 km across India and into the Bay of Bengal, ending with the mass extinction (Keller et al., 2011a, 2012; Keller, this volume).

BIOTIC EFFECTS—PLANKTIC FORAMINIFERA

Planktic foraminifera occupy a wide range of habitats from the surface ocean to subthermocline depths, depending on the chlorophyll maximum zone, temperature, oxygen, and salinity constraints. Large-scale events, such as large igneous province volcanism and very large extraterrestrial impacts, can trigger global climate and environmental changes resulting in high-

stress conditions for marine organisms derived primarily from increased precipitation and acid rain, enhanced weathering, and increased continental runoff (mesotrophy), particularly in nearshore environments, and changes in ocean water chemistry (ocean acidification; Keller, 2003, 2005; Gertsch et al., 2011; Font et al., 2011, this volume; Keller et al., 2011a, 2012). The response of planktic foraminifera depends on species tolerance to environmental changes, reproductive strategies to maximize survival, and the severity, duration, and frequency of perturbations.

Late Maastrichtian to early Paleocene (early Danian) climatic, environmental, and faunal changes have been documented, particularly in planktic foraminifera, for the past three decades and now form a considerable database revealing the biotic responses associated with the environmental stress that culminated in the K-T boundary mass extinction and the subsequent delayed recovery (e.g., Keller et al., 1993, 1995, 2002a, 2002b; Luciani, 1997, 2002; Li and Keller, 1998a, 1998b, 1998c; Kucera and Malmgren, 1998; Olsson et al., 2001; Abramovich and Keller, 2002, 2003; Nordt et al., 2003; Coccioni and Luciani, 2006; Pardo and Keller, 2008; Keller, 2002, 2004; Abramovich et al., 2010, 2011). This has led to the general acceptance that long-term environmental changes preceded and succeeded the K-T boundary mass extinction, despite decades of denial by impact proponents asserting that the Chicxulub impact was the sole cause with no significant ongoing environmental changes (e.g., Olsson et al., 1997; Norris et al., 1999; Lamolda et al., 2005; Arenillas et al., 2000, 2006; Molina et al., 2006; Schulte et al., 2010).

Late Maastrichtian Biotic Stress

Earlier studies suggest that during the late Maastrichtian, optimum planktic foraminiferal assemblages consisted of high species diversity, wide ranges of test sizes, diverse morphologies, and variable degrees of surface ornamentation, forming a continuum from small to large and simple to complex (e.g., Keller, 1988a, 2001; Pardo and Keller, 2008; Keller and Abramovich, 2009; Fig. 4). In these types of polytaxic communities, the diverse, large, complex specialized taxa (K-strategy species) utilize particular food sources, occupy particular ecological niches, have long life spans, and produce small numbers of offspring (Begon et al., 1996, 1998). In contrast, the low-diversity, smaller, less-ornamented species (R-strategists) tolerate a wide range of environments, utilize a variety of food sources, have shorter life spans, and produce larger numbers of offspring. R-strategists

thus optimize chances for survival, whereas K-strategists optimize the good life while it lasts.

With increasing biotic stress, large specialized species are successively eliminated, survivors tend to be dwarfed, and the assemblages are dominated by ecological generalists (R-strategists; Fig. 5; Keller and Pardo, 2004; Keller and Abramovich, 2009). The result is decreasing diversity with increasing biotic stress, which may be due to climate change and/or open marine to successively shallower continental shelf and marginal marine environments. The most extreme biotic stress conditions are interpreted from the dominance of *G. cretacea* and/or *Globoconusa daubjergensis* in low-diversity assemblages (Keller and Pardo, 2004; Pardo and Keller, 2008; Keller and Abramovich, 2009). "Blooms" of these disaster opportunist species indicate an R-selected survival strategy, which is common in unpredictable and stressful environments where quick reproduction improves
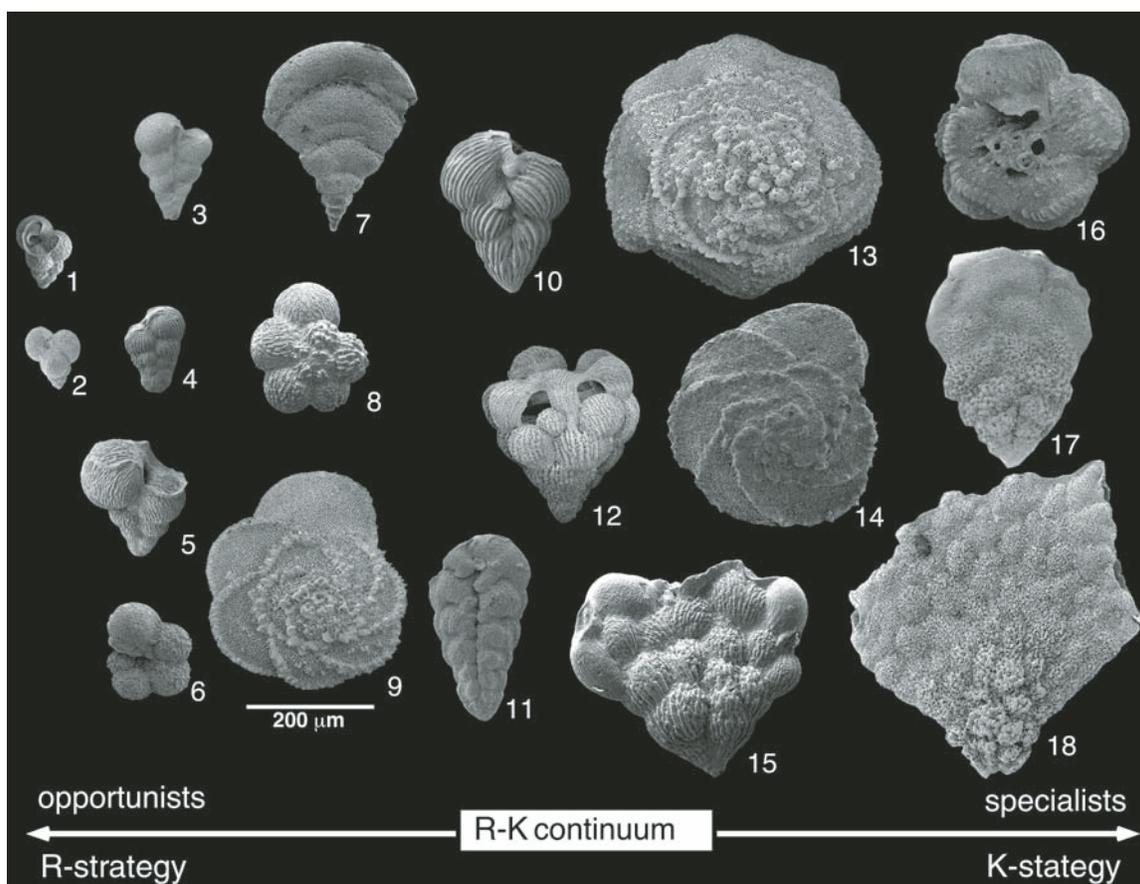
Figure 4. Sizes and shapes of tests of Maastrichtian planktic foraminifera showing a continuum from small R-strategists to large complex K-strategists. R-strategy and opportunistic life of *Guembelitria* are inferred from minute test size, simple chamber arrangement, and isotopically light δ^{13}C values. K-strategy species are inferred from large and complex test morphology, small populations, and heavier δ^{13}C values (modified from Keller and Abramovich, 2009). 1, 2—*Guembelitria cretacea*, 3—*Heterohelix planata*, 4—*Heterohelix navarroensis*, 5—*Heterohelix globulosa*, 6—*Globigerinelloides aspera*, 7—*Pseudotextularia elegans*, 8—*Rugoglobigerina rugosa*, 9—*Globotruncana arca*, 10—*Pseudoguembelina costulata*, 11—*Pseudoguembelina kempensis*, 12—*Racemiguembelina fructicosa*, 13—*Contusotruncana walfischensis*, 14—*Globotruncanita stuarti*, 15—*Planoglobulina acervulinoides*, 16—*Abathomphalus mayaroensis*, 17—*Gublerina cuvillieri*, 18—*Planoglobulina multicamerata*.

the chances of survival. *Guembelitria* species are surface dwellers often associated with unstable environments, mesotrophic conditions of shallow continental shelves, upwelling areas, and regions under volcanic influence (Keller, 2003, 2005, 2011; Keller et al., 2007; reviews in Keller and Pardo, 2004; Pardo and Keller, 2008).

Species dwarfing, or the Lilliput effect, and other morphological deformities are the most easily identified signals of high-stress conditions. Dwarfing is likely a survival response to stress conditions by increasing reproduction rates through early sexual maturation (MacLeod et al., 2000; Keller and Abramovich, 2009). Such faunal responses have been linked to the global rapid climate warming in the latest Maastrichtian, decreased water mass stratification with resultant loss of habitat, high nutrient influx in shallow marine environments, leading to mesotrophic or eutrophic waters with reduced dissolved oxygen content, and reduced symbiotic activity (Abramovich and Keller, 2003; Keller and Abramovich, 2009).

Species richness reflects the actual number of species present in any given sample and is used as proxy for high variability and environmental stress as a function of climate, geography, and ecology (Abramovich and Keller, 2002). The lowest species richness has been consistently observed in areas of volcanic activity, such as in Deep Sea Drilling Project (DSDP) Site 216 on Ninetyeast Ridge, Indian Ocean, in the Neuquén Basin, Argentina, and in the Krishna-Godavari Basin and Meghalaya, India (Keller, 2003, 2005; Keller et al., 2007, 2011a, 2012; Gertsch et al., 2011a). In these regions, species richness varies between 6 and 12 species, but increases in intervals after volcanic activity ceased. We therefore identify extreme global environmental effects correlative with Deccan phase 2 by low species richness/diversity, dwarfing, dominance of disaster opportunists (*G. cretacea*), and variations among other environmentally tolerant small species.

Early Danian Biotic Stress

Significant numbers of small late Maastrichtian species appear to have survived the K-T boundary mass extinction into the early Danian zone P1a, as also testified by their Danian stable isotope signals (e.g., *Heterohelix globulosa*, *Heterohelix planata*, *Heterohelix navarroensis*, *Pseudoguembelina costulata*, *Hedbergella monmouthensis*, *Hedbergella holmdelensis*, *G. cretacea*; Keller, 1988a, 1989a, 1989b; Canudo et al., 1991; Keller et al., 1993, 1994; MacLeod and Keller, 1994; Barrera and Keller, 1990; Keller and Pardo, 2004; Pardo and Keller, 2008; Keller and Abramovich, 2009). However, only *G. cretacea* was a long-term survivor, and it may have been the progenitor of several Danian clades (Fig. 6; Olsson et al., 1999). This species thrived in high-stress environments of the late Maastrichtian as well as in the immediate aftermath of the mass extinction in zone P0 and
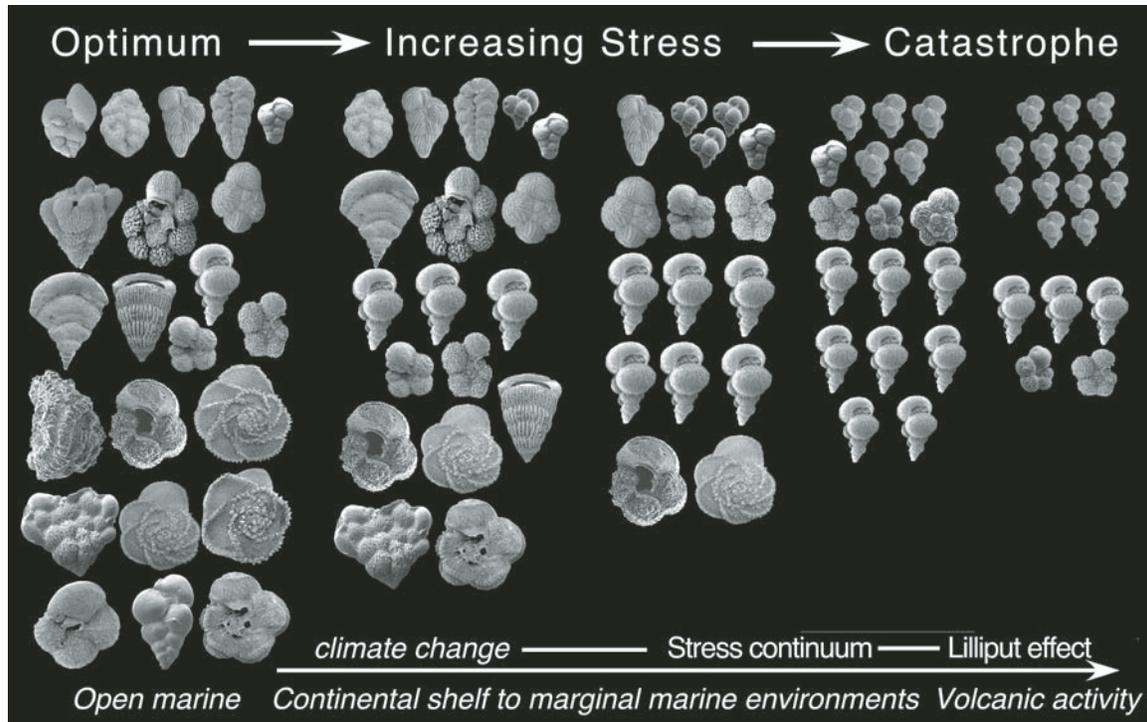

Figure 5. The effects of increasing environmental stress upon planktic foraminiferal assemblages from optimum to catastrophe conditions show the successive elimination of large, specialized K-strategy species, the survival of small R-strategy species, the overall dwarfing of these species, and their great abundance. Figure is modified from Keller and Abramovich (2009).

the lower part of zone P1a, but they decreased in the later part of P1a only to thrive again in P1b. Other survivor species were generally dwarfed in zones P0 and P1a, with *H. globulosa* abundant in shallow-water environments (e.g., Brazos River, Texas, and Nye Klov, Denmark). All survivors rapidly disappeared by the end of P1a (Fig. 6; MacLeod et al., 2000; Keller and Pardo, 2004; Keller and Abramovich, 2009).

All evolving new species found in the early Danian sections are small (generally <100 μm and frequently <63 μm) with thin test walls, small globular chambers, and simple biserial, trise-rial, or trochospiral morphologies (e.g., Keller, 1988a, 1989a; Keller et al., 1993, 1995, 2002a, 2002b; Luciani, 2002; Coccioni and Luciani, 2006; Pardo and Keller, 2008). The first new spe-cies evolved in zone P0 within a few thousand years of the mass extinction (e.g., *Woodringina hornerstownensis*, *Woodringina claytonensis*, *Parvularugoglobigerina extensa*, *Gl. daubjergen-sis*; Fig. 6). Shortly thereafter, in zone P1a, additional small spe-cies evolved with primarily trochospiral coiling (e.g., *Parvularu-goglobigerina eugubina*, *Parvularugoglobigerina longiapertura*,

Eoglobigerina edita, *Eoglobigerina eobulloides*, *Praemurica taurica*, *Globorotalia pentagona*, *Subbotina triloculionoides*, *Parasubbotina pseudobulloides*) and a few biserial morpho-types (*Chiloguembelina midwayensis*, *Chiloguembelina morsei*). Hence, early Danian species diversity remained low and only a few of these species dominated the assemblages in P1a (*P. eugu-bina*, *E. edita*, *W. hornerstownensis*, and other biserial species), suggesting continued high-stress conditions during the 100–200 k.y. after the mass extinction (Fig. 6).

The disappearance of *P. eugubina* and *P. longiapertura* marks the P1a/P1b zone boundary. Throughout zone P1b, spe-cies richness remains low with small simple test morphologies. *Guembelitria* species (*G. cretacea*, *G. irregularis*, *G. danica*, *G. dammula*) dominate yet again, along with *Gl. daubjergensis*, indi-cating a relapse to stressed environmental conditions. A notable recovery to higher diversity, larger test morphologies (>150 μm), and reduced abundance of stress-tolerant species does not take place until zone P1c—long after the K-T boundary mass extinc-tion (Fig. 6).
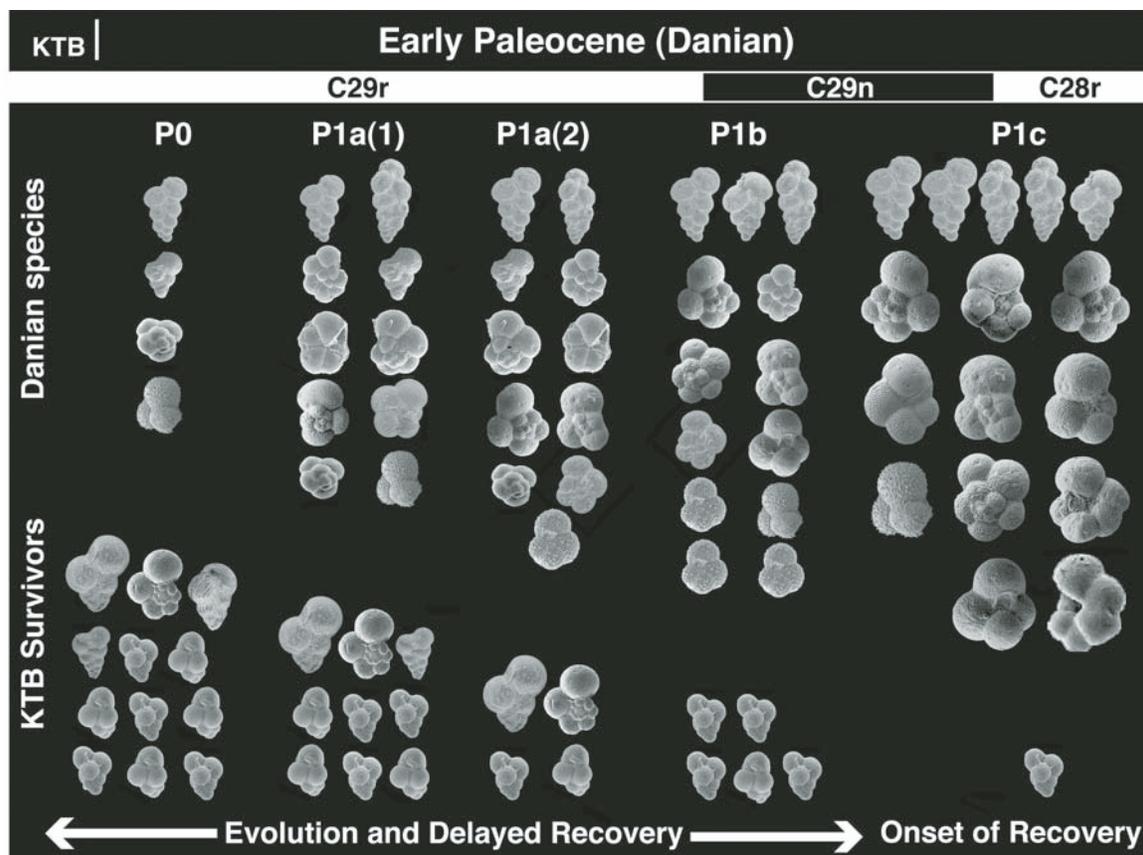
Figure 6. Early Danian evolution and Cretaceous survivor species illustrating the high-stress environment, small dwarfed species, and low diversity that mark the delayed marine recovery through zone P1b. The last phase 3 of Deccan volcanism occurred in zone P1b (C29n). The onset of marine recovery with higher diversity and larger species sizes begins only after Deccan volcanism ended. Note the decreasing abundance of survivor species with increasing evolution and diversity of early Danian assemblages. The number of same specimens qualitatively indicates relative abundance. KTB—Cretaceous-Tertiary boundary.

GLOBAL K-T BOUNDARY DATABASE

This study summarizes the faunal diversity and species abundance data that appear to link high-stress environments during the late Maastrichtian and early Danian to Deccan volcanism phase 2 and phase 3. Over 200 K-T boundary sequences from localities worldwide have been analyzed by one of the authors (Keller), students, and collaborators (Fig. 7). For many of these sections, oxygen and carbon stable isotopes and quantitative planktic foraminiferal analyses are available and make a formidable database with which to test various K-T boundary hypotheses regarding the nature, cause(s), and effects of the mass extinction. The analyzed sections encompass latest Maastrichtian zones CF3, CF2, and CF1 and early Danian zones P0, P1a (subzones P1a[1], P1a[2]), and P1b (correlative with P0, Pα, and P1a of Berggren et al., 1995) (Fig. 8). The database therefore permits evaluation of the Chicxulub and Deccan volcanism–related hypotheses on a global scale (Fig. 7).

We use the high-resolution biozonation that resulted from these studies and was first developed at the El Kef global stratotype section and point (GSSP), refined by additional studies at the nearby Elles section (Keller, 1988a; Li and Keller, 1998a, 1998b; Keller et al., 1995, 2002a; Fig. 8). This biozonation has been tested and successfully applied worldwide, including India (Keller et al., 2008, 2009, 2011a; Malarkodi et al., 2010; Gertsch et al., 2011a). Quantitative species analysis is an integral part of this biozonation and helps with recognition of zones, subzones, and intervals based on species acmes. The biozones and subzones were compared and integrated with lithological characteristics (black clay layer, red oxidized layer with iridium anomaly) and geochemical proxies ($CaCO_3$, total organic carbon [TOC], $\delta^{13}C$).

STABLE ISOTOPES

Late Maastrichtian to early Paleocene (early Danian) environmental changes can be inferred from oxygen and carbon isotopes of well-preserved monospecific planktic and benthic foraminifera and bulk rock sediments. For this review, we used the high-resolution records of the South Atlantic DSDP Site 525A (Li and Keller, 1998a), the Tethys record of Elles, Tunisia (Stüben
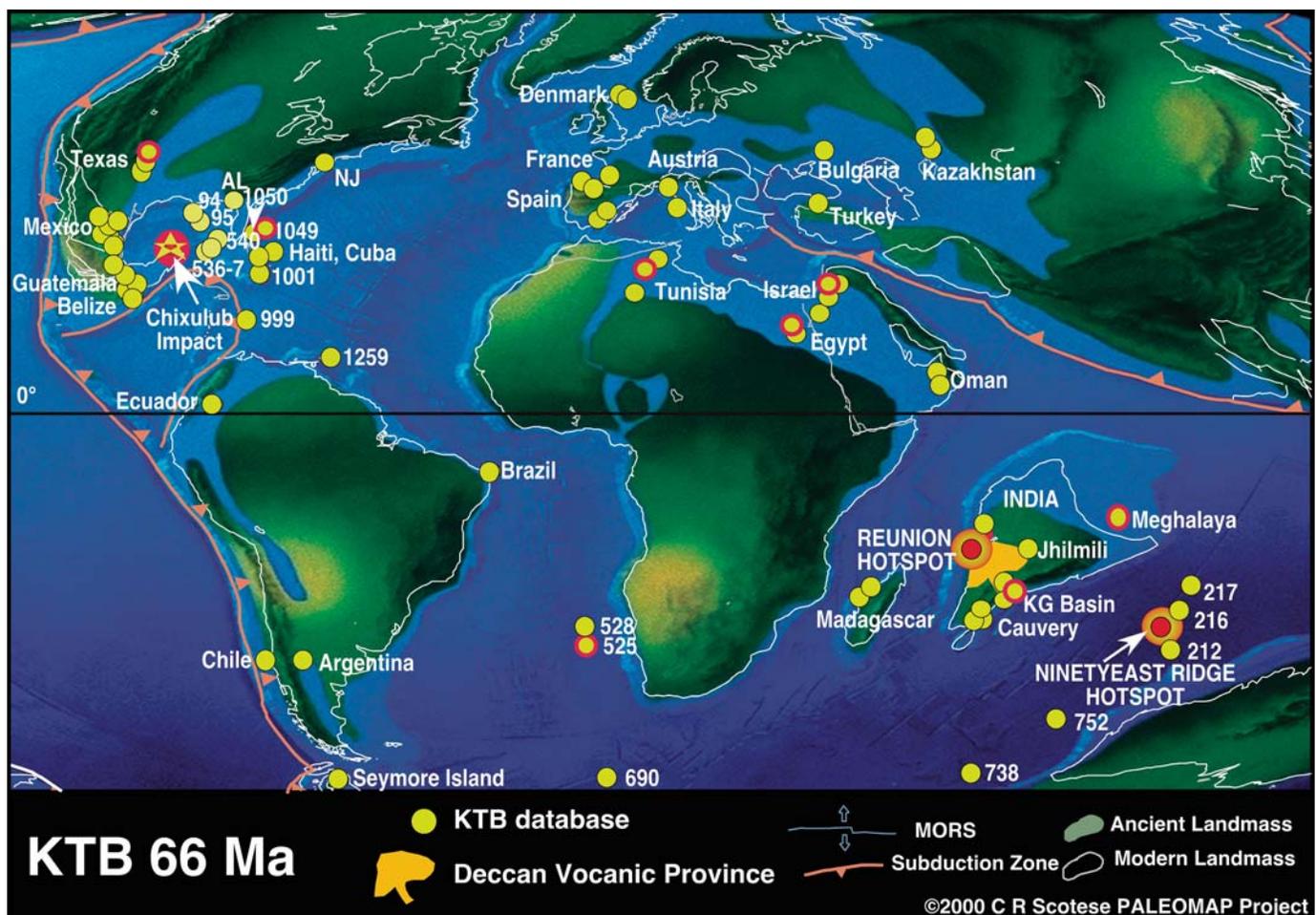

Figure 7. Global database of Cretaceous-Tertiary boundary (KTB) sections studied to date plotted on the paleomap of 66 Ma. Red-circled yellow dots mark sections discussed in this review. MORS—mid-ocean ridges.

Planktic Foraminiferal Biozonations				Biozone Ages		Deccan Volcanism	
Age (Ma) Mag. Polarity	Berggren et al., 1995 Tantawy, 2003	Li & Keller, 1998a, b Keller et al., 1995, 2002a		KTB: 65 Ma Cande & Kent, 1995	KTB: 65.5 Ma Gradstein et al., 2004	Deccan Province	Krishna-Godavari Basin, SE India

Danian

Mag. Polarity / Age	Nannof.	Li & Keller zones	Species	KTB 65 Ma	KTB 65.5 Ma	Deccan	K-G Basin
63.1 / 28N	NP1c	P1c / P1c(2)	*P. trinidadensis* / *P. inconstans*	P1c ~1.47 my	P1c ~1.33 my		Full marine recovery
64.12 / 64.43 / NP1b	P1b / P1c(1)	*S. varianta*				
29N / 65	NP1a	P1a / P1b		P1b ~670 ky	P1b ~590 ky	Phase-3	Phase-3 megaflows
65.12		Pα / P1a / P1a(2) / P1a(1)	*P. eugubina* / *P. pseudobull.* / *P. eugubina* / FA Danian spp.	P0 + P1a 260 ky	P0 + P1a 380 ky	KTB	high stress and delayed recovery; Phase-2 megaflows
29R / 65.5	P0	P0 / CF1 / CF2	*P. hantkenin.*	65.0–65.3 300 ky	65.5–65.66 160 ky	Phase-2	KTB mass extinction

U. Maastrichtian

Mag. Polarity / Age	Nannof.	Li & Keller zones	Species	KTB 65 Ma	KTB 65.5 Ma	Deccan	K-G Basin
M. prinsii							
65.86 / 66	*M. murus*	CF3 *P. hariaensis*	CF2 / *G. gansseri*	65.3–65.45 150 ky	65.66–65.78 120 ky		onset of mass extinction
				65.45–66.83 1.43 my	65.78–66.99 1.21 my		
30N / 67	*N. freque.*		*P. hariaensis*				onset of intense volcanism in the Krishna-Godavari Basin
		CF4 *R. fructicosa*		66.83–68.33 1.50 my	66.99–68.36 1.37 my	Phase-1	
68 / 31N							

A. mayaroensis 65.5–68.72

Figure 8. Late Maastrichtian and early Danian planktic foraminiferal zonal schemes and ages of biozones calculated based on two time scales with the Cretaceous-Tertiary boundary (KTB) at 65.0 and 65.5 Ma. The stratigraphic position of Deccan megaflows and the onset of the Cretaceous-Tertiary boundary mass extinction in the Krishna-Godavari Basin are based on Keller et al. (2011a). This review concentrates on the shaded interval. Index species: *Nephrolithus frequens, Micula murus, Micula prinsii* (nannofossils)*; Racemiguembelina fructicosa, Planoglobulina hariaensis, Gansserina gansseri, Plummerita hantkeninoides, Parvularugoglobigerina eugubina, Parasubbotina pseudobulloides, Subbotina varianta, Praemurica inconstans, Praemurica trinidadensis* (planktic foraminifera).

et al., 2003), and the shallow shelf record of Brazos, Texas (Mullinax-1 core; Abramovich et al., 2011). At all three localities, foraminiferal test preservation varies from excellent (Brazos, Texas) to well preserved (DSDP Site 525A, Elles, Tunisia).

Late Maastrichtian

South Atlantic DSDP Site 525A

Remarkable climate changes occurred during the last 280 k.y. (zones CF2 and CF1) of the Maastrichtian, as shown in the high-resolution records (samples analyzed at 2000–5000 yr intervals) of the middle-latitude South Atlantic (Walvis Ridge DSDP Site 525A; Fig. 9; Li and Keller, 1998a). At Site 525A, the long-term global cooling trend that began in the late Campanian ended with the maximum Cretaceous cooling near the base of chron C29r, correlative with the CF3-CF2 zones transition. In the following

warm event, bottom waters warmed rapidly by 3–4 °C (0.8‰ decrease in benthic $\delta^{18}O$ values near the base of CF2). This deep-water warming trend was interrupted by a short cooling event (1 °C) and ended in the upper part of CF1, when climate cooled rapidly by 2–3 °C (0.5‰ increase in benthic $\delta^{18}O$ values; Fig. 9). In contrast to the more stable deep-water temperatures, planktic $\delta^{18}O$ values of surface waters (*Rugoglobigerina rugosa*) strongly fluctuated during the warm event (0.3‰–0.5‰), suggesting unstable climatic conditions, although some of this variation could also be attributed to diagenetic effects and/or variations in species habitats. Both surface- and deep-water $\delta^{13}C$ values remained relatively steady through the warm event, fluctuating ~0.3‰, but they significantly increased during the subsequent cooling in the upper zone CF1 (Fig. 9). The late Maastrichtian record at Site 525A ends at the K-T boundary hiatus with an indeterminate interval eroded (Li and Keller, 1998a, 1998b).
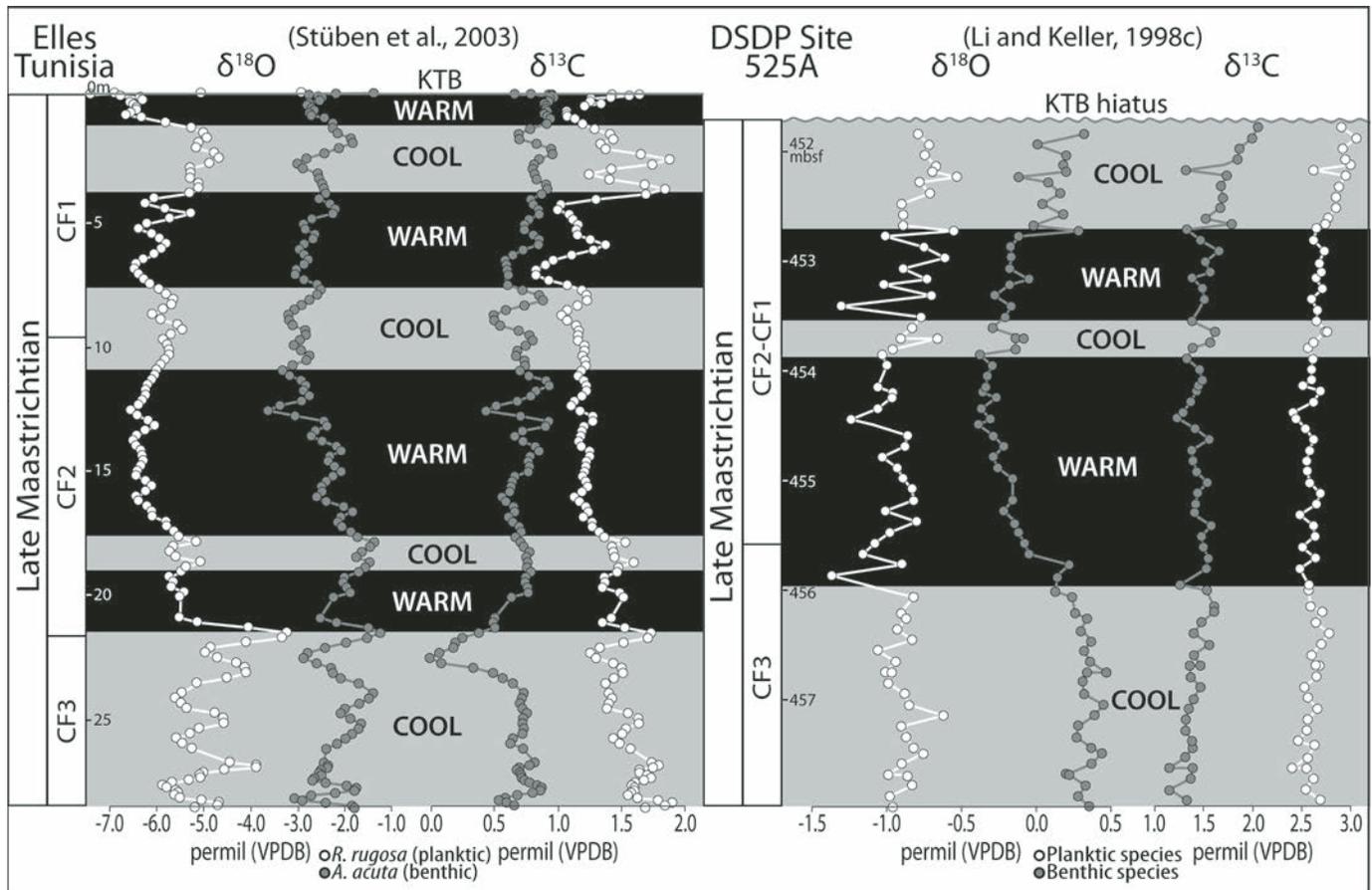
Figure 9. Carbon and oxygen isotopes of monospecific planktic and benthic foraminifera at Elles, Tunisia, and South Atlantic Deep Sea Drilling Project (DSDP) Site 525A. Gray marks cool intervals; black marks warm intervals. Note the broad climate warming of zones CF1–CF2 at Site 525A shows a more complex pattern at Elles, where two warm phases are separated by a short cool pulse. The late Maastrichtian warming at Elles is not present at Site 525A, probably because of the Cretaceous-Tertiary boundary (KTB) hiatus. Note that at Elles, oxygen isotope values are 3‰–4‰ lighter, suggesting diagenetic effects due to burial diagenesis and/or interaction with isotopically light meteoric water as a result of freshwater input. Data are from Li and Keller (1998a) and Stüben et al. (2003). VPDB—Vienna Peedee belemnite; planktic species—*Rugoglobigerina rugosa*; benthic species—*Anomalinoides acuta*, now known as *Cibicidoides pseudoacuta*.

Elles, Tunisia

In the middle-shelf section of Elles, Tunisia, samples were analyzed at 5–10 cm intervals, recording a sample resolution of ~2000 yr (Stüben et al., 2003). Oxygen isotope values are 3‰–4‰ lighter than at Site 525A (Fig. 9), suggesting freshwater influx and diagenetic effects due to burial diagenesis and/or interaction with isotopically light meteoric water (Stüben et al., 2003). This prevents the calculation of actual paleotemperatures, although climate trends are likely preserved, as indicted by their similarity to Site 525A. Significant differences are largely due to the expanded Elles record of 22 m, compared with just 4.2 m at Site 525A, and the lower-latitude location. As a result of this expanded record and detailed sampling, the climate changes are better resolved in both surface and bottom waters.

Three significant cool intervals can be recognized in planktic and benthic oxygen isotopes: lower part of CF2, base of CF1, and upper part of CF1 (Fig. 9). Only the upper two cool intervals are

recognized in Site 525A. In addition, there is significant warming in the top meter immediately preceding the K-T boundary, which is not present at Site 525A due to a hiatus. Surface waters show less sample variability in δ18O values and four distinct strong warm events (Fig. 9). The δ13C values at Elles are significantly more variable than at Site 525A. In zone CF3, both surface and bottom waters show a gradual decrease, but the latter shows an abrupt 0.7‰ shift near the top of CF3. During the following warm event, the bottom-water δ13C values gradually increase up to the K-T boundary. In contrast, surface δ13C values decrease through the warm event, temporarily increase in the lower half of the subsequent cooling, and rapidly increase just below the K-T boundary (Fig. 9).

Brazos River, Texas

At the Brazos section (core Mullinax-1), samples were analyzed at 5–10 cm intervals (Abramovich et al., 2011). The

sediment accumulation rate for the CF2–CF1 interval is relatively high (9 m) compared with Site 525A (4.2 m), though less than at Elles (22 m). However, this excludes erosion at the base of the sandstone complex, which is estimated to be several meters. Preservation of foraminiferal tests is excellent, which rules out significant diagenetic alteration. However, $\delta^{18}O$ and $\delta^{13}C$ values covary and are ~2‰–3‰ lighter than at Site 525A. This has been attributed to the shallow shelf location and influx of freshwater during warm intervals (Abramovich et al., 2011). Therefore, no temperatures calculations were made for Brazos.

Compared with deep-water environments, climate changes recorded in shallow nearshore environments can be expected to show more enhanced temperature changes modified by proximity to land. This is evident in the Mullinax-1 core, where $\delta^{18}O$ values vary by 2‰–3‰ (Fig. 10). The warm/cool climate spans the same interval from the CF3-CF2 transition to the K-T boundary, but there are significant differences in the timing relative to Elles. This may be largely due to the rarity of the zone CF1 and CF2 index species (first appearance of *Plummerita hantkeninoides*, last appearance of *Gansserina gansseri*; Fig. 8) at Brazos and hence uncertainty in the CF3-CF2 and CF2-CF1 boundary placements.

At Brazos, the first warm event (CF3-CF2 transition) is significantly shorter than at Elles, which may be due to erosion or nondeposition, which commonly accompanies the maximum cooling and sea-level regression near the end of CF3. The second warm event shows highly fluctuating values with freshwater influx (Fig. 10; Abramovich et al., 2011). The subsequent cool interval marks a sea-level fall, erosion, and deposition of the sandstone complex with reworked Chicxulub impact spherules (Adatte et al., 2011; Keller et al., 2011b). Claystone deposition resumes above the sandstone complex as sea level rises and temperatures gradually increase toward the K-T boundary (Fig. 10). Bulk $\delta^{13}C$ values decrease during the pre–K-T boundary warming (Keller et al., 2007), which is contrary to the increase observed at Elles.

Timing of Climate Change

We can derive best estimates for the age and duration of the major climatic changes based on sediment accumulation rates calculated from the expanded Elles section. We use the time scale of Gradstein et al. (2004), which places the K-T boundary at 65.5 Ma, and zones CF1 and CF2 span the last 160 k.y. and 120 k.y., respectively, corresponding to most of chron C29r at the top of the Maastrichtian. Rapid climate warming began ~280 k.y. before the K-T boundary and reached its maximum near the top of zone CF2, or within ~110 k.y. (including the short cooling in the lower part of CF2; Fig. 9). The subsequent cool and warm intervals span ~50 k.y. and 60 k.y., respectively, followed by another cool interval of ~40 k.y. and the latest Maastrichtian warming (~20 k.y.). Although these values are tentative, they demonstrate that the warm and cool intervals were of relatively short duration.

Early Danian Climate Change

The early Danian is a difficult time interval for evaluation of climatic and environmental changes because the K-T boundary transition is frequently incomplete with hiatuses (MacLeod and Keller, 1991a, 1991b; Keller et al., 2013), which makes comparison of isotope records difficult. In addition, few high-resolution Danian records exist, and most studies have concentrated only on the K-T boundary and its immediate aftermath. We examined the published records concentrating on zones P1a and P1b (zonal scheme by Keller et al., 1995, 2002a; Fig. 8). Because of frequent hiatuses at the K-T boundary, the earliest Danian stable isotope record is not well understood in zone P1a and at the P1a-P1b boundary, and the climatic and environmental history of this interval is still uncertain. However, for zone P1b, the sediment record is generally well represented, and we concentrate on this interval.

The most detailed early Danian record for zone P1b is from the North Atlantic Ocean Drilling Program (ODP) Site 1049C,
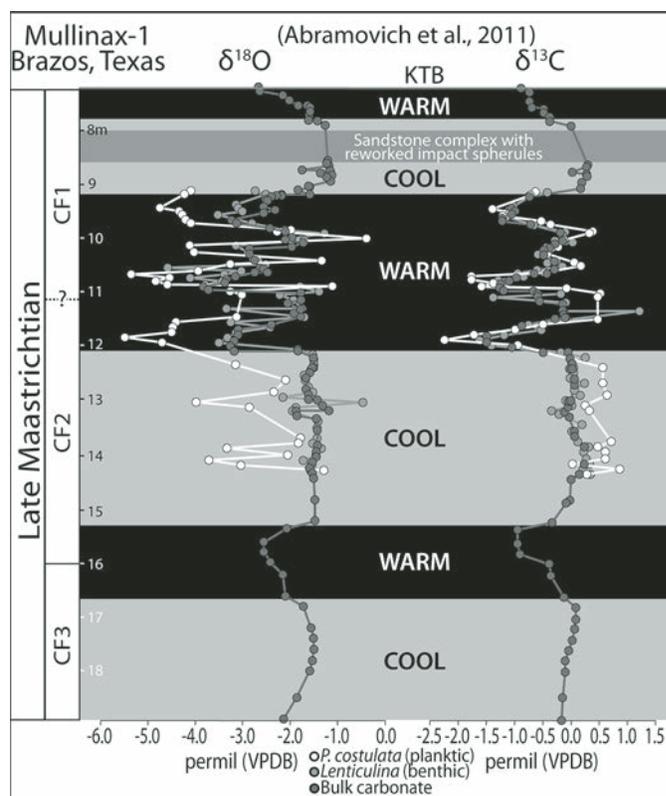
Figure 10. Oxygen and carbon isotope data from monospecific planktic and benthic foraminifera and bulk rock at the Brazos River, Texas, Mullinax-1 core. Note the late Maastrichtian CF2–CF1 warming phases are similar to Elles with two main warm intervals plus the end-Maastrichtian warming. Note: the very negative $\delta^{18}O$ values likely reflect freshwater influx during warm phases. Data are from Abramovich et al. (2011). KTB—Cretaceous-Tertiary boundary; VPDB—Vienna Peedee belemnite; planktic species—*Pseudoguembelina costulata;* benthic species—*Lenticulina.*

Effects of Deccan volcanism on paleoenvironment and planktic foraminifera: A global survey

where Quillévéré et al. (2008) recorded two short-term negative δ18O and δ13C excursions that define the Dan-C2 event (~1.5‰; Fig. 11). Sea-surface temperature rose an estimated ~4 °C, as suggested by the ~1‰ shift in the planktic foraminifer *Praemurica taurica*, assuming that samples are not biased by postdepositional processes. Similar excursions were recorded at South Atlantic Sites 527, 528, Italy and Ukraine, suggesting a global event (Quillévéré et al., 2008; Coccioni et al., 2010; Gilmour et al., 2013).

However, available isotope records from the eastern Tethys (Israel, Egypt) do not mirror the structure or position of the Dan-C2 isotope event at Site 1049C, although distinct excursions are present (Fig. 11). In all eastern Tethys sections, the first δ18O and δ13C excursions are at or near the P1a-P1b boundary. The second excursion, which likely reflects the Dan-C2 event, occurs significantly above this interval, although the characteristic double-peak excursion of Site 1049C is not recognized. Several factors can explain these differences, including the presence of hiatuses and low sample resolution. All eastern Tethys sections, as well as North Atlantic Site 1049C, have multiple early Danian hiatuses, including at the K-T boundary, with most of zone P1a missing, and at the P1a-P1b boundary, with the lower part of zone P1b and upper part of zone P1a eroded (Keller and Benjamini, 1991; Keller et al., 2002a, 2013; Punekar et al., 2014). This can explain the variable stratigraphic position of the isotope excursion referred to as Dan-C2.

BIOTIC STRESS—LATE MAASTRICHTIAN

Biotic stress conditions associated with the late Maastrichtian climate warming and cooling have been documented in numerous localities, summarized in Pardo and Keller (2008) and Keller and Abramovich (2009). Here, we review the climatic and environmental effects on planktic foraminiferal species diversity and abundances based on high-resolution quantitative studies from the middle-latitude South Atlantic (Li and Keller, 1998a; Abramovich and Keller, 2003), the eastern Tethys (Abramovich and Keller, 2002; Stüben et al., 2003), and Western Interior Seaway (Texas; Abramovich et al., 2011; Keller, 2011).

DSDP Site 525A—South Atlantic

The biotic response to the late Maastrichtian climate warming in the South Atlantic Site 525A includes dwarfing, decreased diversity, temporary disappearance of species, decreased photosymbiotic activity, and depth migration (Fig. 12; Abramovich and Keller, 2003). The biotic stresses appear to be primarily associated with temperature-related changes in the water mass
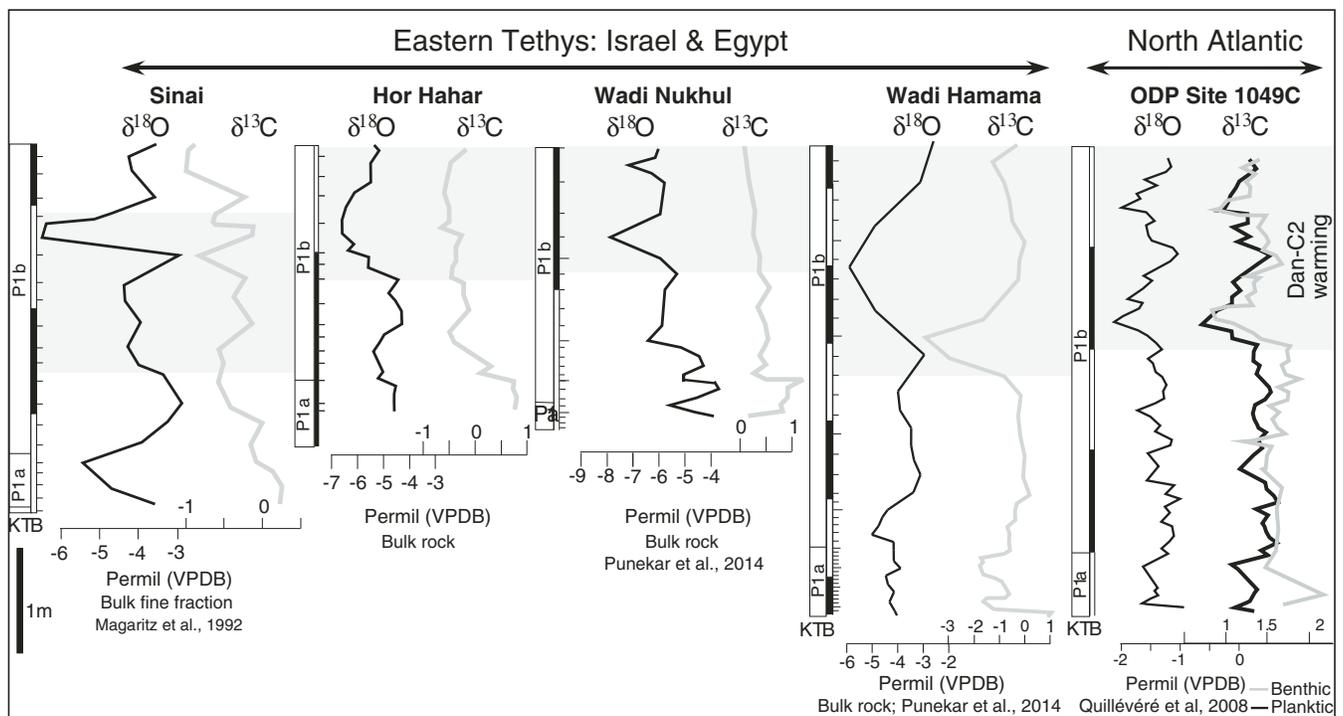
Figure 11. Oxygen and carbon isotope data (planktic, benthic, and bulk rock) in sections from the North Atlantic (Ocean Drilling Program [ODP] Site 1049C) and eastern Tethys (Israel and Egypt). Coeval zone P1b excursions (gray shaded area) originally identified at Site 1049C as Dan-C2 event (Quillévéré et al., 2008) are present but do not mirror the characteristic double-peak structure. The reason is likely low sample resolution. KTB—Cretaceous-Tertiary boundary; VPDB—Vienna Peedee belemnite.

stratification accompanied by decreased niche habitats for specialized large species.

The typical small (63–150 μm) middle-latitude species were least affected and retained their population sizes, with the exception of the dominant *Heterohelix planata* (formerly known as *Heterohelix dentata*), which decreased significantly during warm intervals and increased during cool intervals. *Heterohelix globulosa* is less abundant but also increased during the cooling near the end of the Maastrichtian. In contrast, the disaster opportunist *G. cretacea* is rare.

Dwarfing is the most striking response to the stress conditions associated with climate warming. All morphotypes are affected (Fig. 12), particularly the large (>150 μm), complex, specialized species living at intermediate depth (thermocline). Stressed assemblages show 30%–60% of the population dwarfed to one-third or half of their normal average size.

The Shannon-Weaver index (H′; Buzas and Gibson, 1969) for species diversity shows major changes at Site 525A. For large species (>150 μm), diversity drops dramatically at the onset of warming and recovers partly during cool intervals but never regains the prewarming high diversity (Fig. 12). The reason for this diversity drop is the high number and high abundance of dwarfed larger species to sizes below 150 μm.

Elles, Tunisia—Western Tethys

The faunal turnovers in the middle-latitude South Atlantic and Tethys Oceans are broadly similar, though *H. globulosa* dominates in the Tethys. *Heterohelix planata* mirrors the pattern at Site 525A, with greater abundance during cool intervals and decreased abundance (from ~30% to ~10%) during warm intervals (Fig. 13). *Heterohelix globulosa* shows a general decline during warm intervals, although this relationship is not very consistent. Increased abundances of *G. cretacea* are observed in zones CF3 and CF1, though abundances are too low to compare with shallower shelf sequences where this species dominates (Keller and Pardo, 2004; Pardo and Keller, 2008). Complex species, such as the intermediate-dwelling globotruncanids, decrease in their relative abundance during cool intervals with a slight recovery during warming.

Diversity trends at Elles are different from Site 525A. The values of the diversity index H′ for small (63–150 μm) and large (>150 μm) species show parallel trends. During cool intervals in zones CF3, CF2, and CF1, diversity of large species drops, and diversity of small species increases (Fig. 13). During the first two warm intervals, diversity of the large species is higher than that of small species. The main decrease begins in the
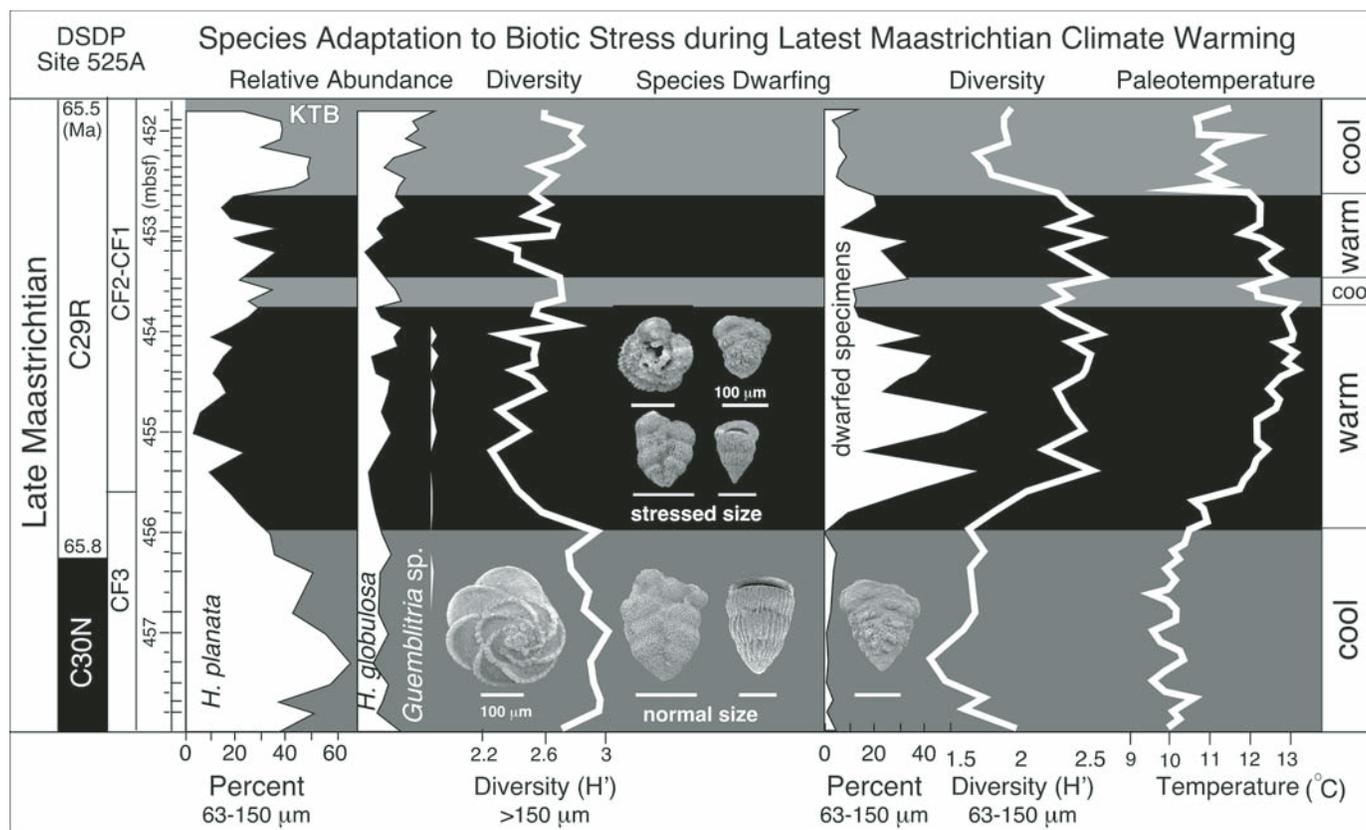

Figure 12. Species adaptation to biotic stress during the late Maastrichtian climate warming at Deep Sea Drilling Project (DSDP) Site 525A, modified from Li and Keller (1998a) and Abramovich and Keller (2003). KTB—Cretaceous-Tertiary boundary; *H. planata—Heterohelix planata*, *H. globulosa—Heterohelix globulosa*.

warm interval near the top of zone CF2 and continues into the first cooling of zone CF1, reaching minimum values along with small species. During the CF1 warm and cool intervals up to the K-T boundary, small species diversity is slightly higher than for large species. Diversity H′ for larger species thus indicates high-stress conditions beginning near the top of zone CF2, whereas for small species, diversity increases. In contrast, at Site 525A, dwarfing of larger species resulted in significant diversity reduction (Fig. 12). The diversity decrease in the CF1 cool intervals likely reflects the decreased abundance or absence of specialized large species living at thermocline depths, possibly due to upwelling effectively reducing habitat space. This can be evaluated based on species richness.

All variability in species richness is observed in intermediate-depth dwellers (the thermocline dwellers; Abramovich and Keller, 2003; Abramovich et al., 2003), which increase in diversity during warming and decrease during cooling, indicating major changes in the water mass stratification (Fig. 13). These changes may be related to upwelling and reduced thermocline depth during cooling and expansion of the oxygen minimum zone during warming. Both cooling and warming would

have placed maximum stress on the intermediate-dwelling large specialized species, driving them to near extinction. Specialized species show normal combined species diversity (66%) but very low combined total species abundances (<10% overall, <5% globotruncanids). Surface- and deep-water dwellers experienced little variability.

Brazos River, Texas—Western Interior Seaway

For most of the late Maastrichtian, claystone deposition in the Brazos River area occurred in a middle shelf environment, which dropped to inner shelf depth in the upper part of zone CF1, marked by an unconformity and deposition of the sandstone complex with reworked Chicxulub impact spherules (Fig. 14; Keller et al., 2007, 2011b). Claystone deposition resumed with latest Maastrichtian zone CF1 assemblages and stable isotope signals marking deposition of the sandstone complex and the reworked Chicxulub impact spherules as latest Maastrichtian in age.

The same small heterohelicids (*H. planata*, *H. globulosa*) and *Guembelitria* that dominate at Elles and Site 525A dominate at Brazos. These three species account for 75%–95% of the
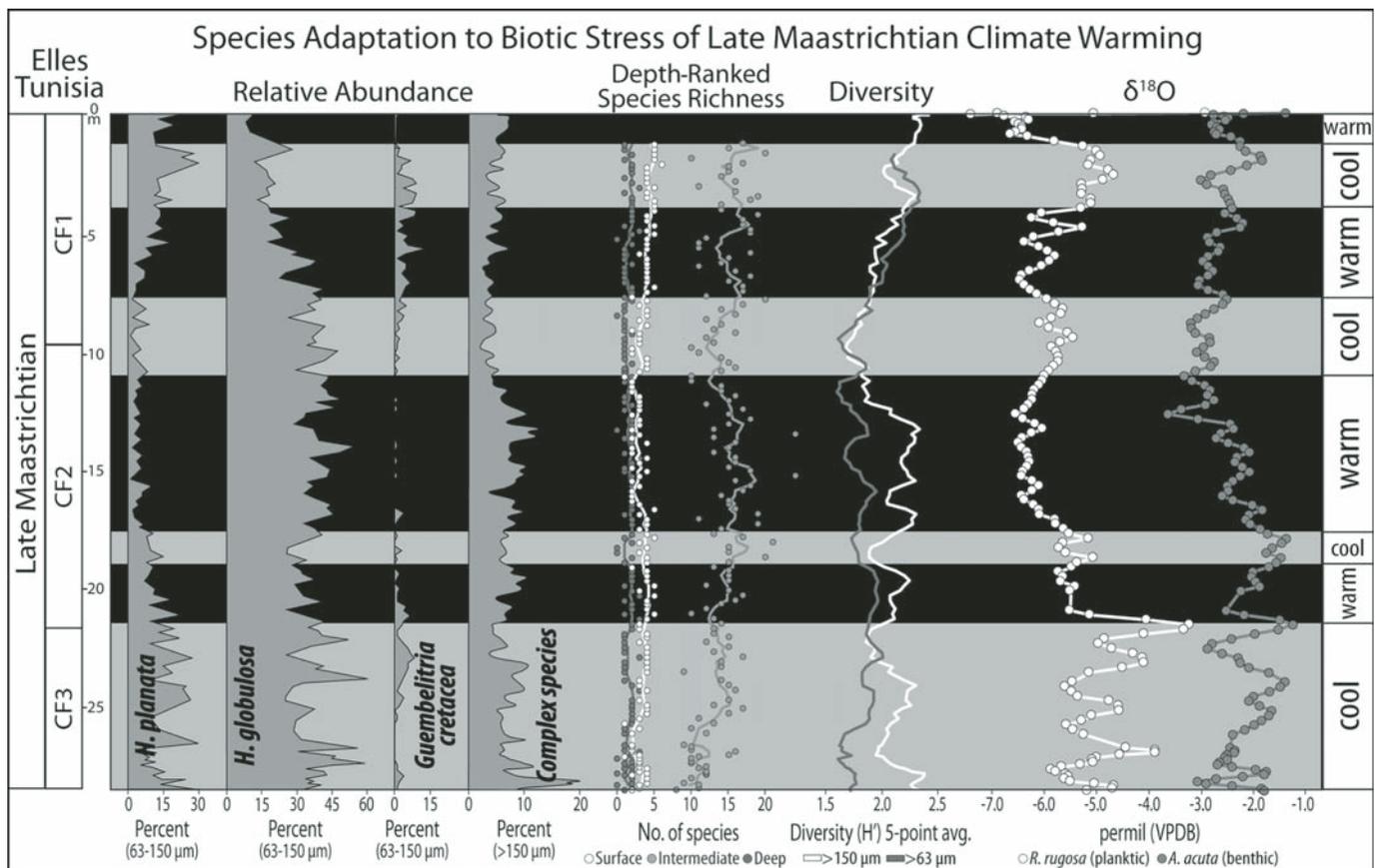

Figure 13. Species adaptation, species richness, and diversity compared with oxygen isotope trends at Elles, Tunisia. Data are from Abramovich and Keller (2002) and Stüben et al. (2003). VPDB—Vienna Peedee belemnite; *H. planata—Heterohelix planata*; *H. globulosa—Heterohelix globulosa*.

total planktic foraminiferal population (Fig. 14; Abramovich et al., 2011; Pardo and Keller, 2008). *Heterohelix planata* shows a distinct preference for cooler temperatures with major decreases in relative abundances in both warm phases, similar to Elles and Site 525A. In the first warm phase (CF3-CF2 transition), relative abundance drops from 50% to 25%, but it recovers during the subsequent cooling. Interestingly, the terminal population decrease begins in the middle warm interval (zone CF1), with no recovery in the subsequent cooling. *Heterohelix globulosa* shows the opposite trend, with higher abundances during the warm intervals and continuing high abundance across the K-T boundary into the early Danian. Species are dwarfed in zone CF1 as well as in the early Danian zones P0–P1a, where survivor populations of *H. globulosa* show Danian isotope signals (Barrera and Keller, 1990; MacLeod et al., 2000). The most abundant species during CF1 warming is *G. cretacea*, with pronounced peaks (>50%) at the warm-cool transitions.

The diversity index H′ shows little change except for a gradual decrease through the latest Maastrichtian. Species richness plotted as histograms for small and large species for each

meter interval shows larger species disappearing in cool intervals and particularly during deposition of the sandstone complex (Fig. 14). This is due to the sea-level drop to inner neritic depths and even subaerial exposure within 2.5 km of Mullinax-1, which excluded all but the surface dwellers from the area (Keller et al., 2011b; Adatte et al., 2011). Species richness (5 point average) fluctuates with climate changes, showing maxima during warm phases and minima during cool phases, as also observed at Elles.

BIOTIC STRESS—EARLY DANIAN

The planktic foraminifera during the early Danian indicate prolonged environmental stress and delayed ecosystem recovery after the mass extinction. The most expanded early Danian sequences known to date are from Tunisia (Elles and El Kef sections) and Texas (Brazos River sections). However, high-resolution stable isotope records and faunal analyses for zones P1b and P1c are still lacking. In the condensed and less complete sequences from the North and South Atlantic (D'Hondt and Keller, 1991; Keller, 1993; Keller et al., 2013) and the eastern Tethys (Fig.
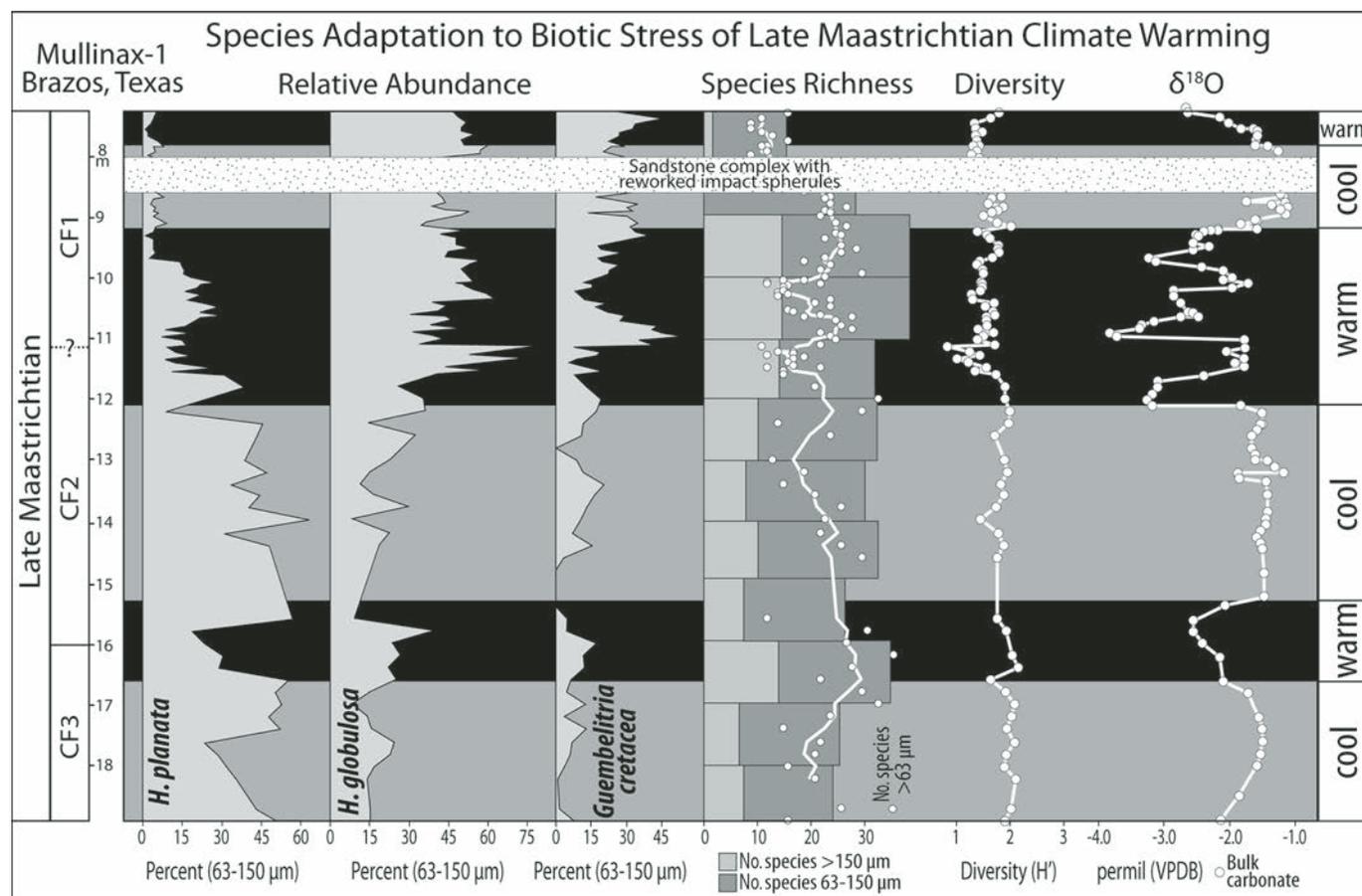

Figure 14. Species adaptation, species richness, and diversity compared with oxygen isotope trends at Brazos, Texas. Note the distinct changes with warm/cool events. Data are from Abramovich et al. (2011). VPDB—Vienna Peedee belemnite; *H. planata—Heterohelix planata*; *H. globulosa—Heterohelix globulosa*.

15), early Danian zones P0 and P1a contain multiple hiatuses (MacLeod and Keller, 1991a, 1991b; Keller and Benjamini, 1991; Keller et al., 2013; Punekar et al., 2014). For this reason, we concentrate on zone P1b, which is relatively complete.

Guembelitria blooms are well known from the aftermath of the K-T boundary mass extinction, but their reappearance in zone P1b (frequently with blooms of *Gl. daubjergensis*) is less well documented. In most sections in Israel and Egypt, the P1b *Guembelitria* blooms begin near the P1a-P1b hiatus, correlative with a major isotope excursion at Hor Hahar and Wadi Hamama (Figs. 11 and 15). Species richness remains low, and species are dwarfed through zone P1b (10–15 species; e.g., Keller and Benjamini, 1991; Keller, 1988a, 1988b, 2002, 2004; Punekar et al., 2014). Near the top of P1b, *Guembelitria* blooms decrease rapidly and are replaced by blooms of chiloguembelinids, which in turn give way to the first larger (>150 μm) trochospiral species morphologies and higher diversity in zone P1c. This marks the onset of full marine recovery after the mass extinction.

This pattern of *Guembelitria* blooms, frequently accompanied by blooms of *Gl. daubjergensis*, is observed from India to the Tethys and Atlantic to Texas, marking global high-stress environments in open marine and marginal marine settings (Figs. 16 and 17). These renewed high-stress conditions follow a period of

recovery in the upper part of the *P. eugubina* zone (P1a[2]), as indicated by the low or nearly disappearing *Guembelitria* species (Fig. 17). Interestingly, the onset of the renewed high-stress environment is marked by the extinction of *P. eugubina* and its similar morphotype *P. longiapertura*, as well as changes in the relative abundances of other species (Fig. 15) documented in numerous publications (e.g., Keller, 1988a, 1989a, 1989b; Keller and Benjamini, 1991; Canudo et al., 1991; Keller et al., 2013; Punekar et al., 2014). The renewed high-stress environment and long-delayed marine recovery after the mass extinction have long been an enigma and largely ignored by paleontologists. Recent documentation of early Danian zone P1b assemblages in intertrappean sediments between Deccan lava megaflows in India provides clues to this mystery.

DECCAN VOLCANISM AND THE K-T BOUNDARY MASS EXTINCTION

Recent studies of deep wells in the Krishna-Godavari Basin of India have documented the K-T boundary mass extinction in marine sediments between Earth's largest megaflows, reaching >1000 km across India during the main Deccan eruption phase 2 (80% of total Deccan volume) in the latest Maastrichtian chron

Figure 15. Dominant species populations in the early Danian zones P1b and P1c in the eastern Tethys. Note the blooms of ecological opportunists *Guembelitria* and *Globoconusa* during zone P1b, indicating maximum high-stress environments for planktic foraminifera correlative with Deccan volcanism phase 3. KTB—Cretaceous-Tertiary boundary.

Figure 16. *Guembelitria* stress events in zone CF1 and P1b correlative with Deccan volcanic phase 2 and phase 3 of the late Maastrichtian and early Danian of continental shelf sequences from India through the Tethys, North Atlantic, and Texas. Maximum stress observed in the latest Maastrichtian of NE India (Meghalaya) decreases westward. In contrast, *Guembelitria* blooms in the early Danian zone P1b remain high across the oceans. K—Cretaceous; T—Tertiary; *G. daubjergensis*—*Globoconusa daubjergensis*; *G. cretacea*—*Guembelitria cretacea*.

Effects of Deccan volcanism on paleoenvironment and planktic foraminifera: A global survey

Figure 17. *Guembelitria* blooms in open marine environments show similar distributions and abundances in the early Danian zone P1b, but only minor *Guembelitria* blooms in the latest Maastrichtian zone CF1. K—Cretaceous; T—Tertiary.

C29r (zones CF1–CF2; Chenet et al., 2007, 2008; Self et al., 2008; Keller et al., 2011a, 2012). These data now permit re-evaluation of the climatic changes and global high-stress conditions in zones CF1–CF2 before the K-T boundary mass extinction that could never be explained by the Chicxulub impact hypothesis.

The expanded paleoclimatic records from Tunisia and Texas with distinct multiple rapid warm-cool events suggest that climatic changes in the late Maastrichtian zones CF1–CF2 were complex and episodic (Figs. 9 and 10), rather than a single global hyperthermal event in chron C29r, as originally identified at Site 525A and elsewhere (Fig. 9; Li and Keller, 1998a; Ravizza and Puecker-Ehrenbrink, 2003; Nordt et al., 2003; MacLeod et al., 2005; Robinson et al., 2009). The apparently single hyperthermal event can be explained by condensed sedimentation at Site 525A and elsewhere, as evident by comparison with Tunisia and Texas,

where sediment accumulation is two to three times higher. The rapid paleoclimatic fluctuations evident in the carbon and oxygen isotope records point toward recurrent environmental perturbations, which likely resulted from the rapid succession of major Deccan eruptions, particularly the four lava megaflows that span planktic foraminiferal zones CF1–CF2 and most of the *Micula prinsii* nannofossil zone in the Krishna-Godavari Basin (Keller et al., 2011a, 2012). In the sediments below the first megaflow, planktic foraminifera gradually suffered a nearly 50% drop in species richness due to volcanic activity in the central magmatic province, as indicated by geochemical and mineralogical data (Keller et al., 2012). In the intertrappean sediments after the first megaflow eruption, survivors suffered another nearly 50% drop, leaving only 7–8 species. No recovery occurred between the next three megaflows, and the K-T boundary mass extinction was

complete by the end of the last megaflow of phase 2. Whether this extinction pattern in India can be recognized globally remains to be examined in high-resolution expanded sediment records. Keys to this endeavor are complete K-T boundary sequences with high sediment accumulation rates, good carbonate preservation, and high-resolution stable isotope records, and ideally the recognition of unique chemical markers of Deccan volcanism.

Robinson et al. (2009) have linked a decline in [187]Os/[188]Os beginning at the C30n-C29r transition and the late Maastrichtian global warming event with the main phase 2 of Deccan volcanism. Font et al. (2011, this volume) discovered a promising technique for identifying Deccan volcanism signals based on magnetic studies at Bidart (France) and Gubbio (Italy), where Cl-bearing iron oxides in low-magnetic-susceptibility (MS) intervals just below the K-T boundary suggest a reaction between HCl-rich volcanic gas and liquid-solid aerosols. Detailed faunal analysis of the Bidart section reveals that this low MS interval spans the last 30 cm of zone CF1. The planktic foraminifera here are few and poorly preserved due to dissolution, marking ocean acidification linked to Deccan volcanism (Font et al, 2011). Sial et al. (2013) used mercury concentrations as a proxy for volcanic activity and determined the atmospheric Hg and CO_2 buildup in three K-T boundary localities (Argentina, Brazil, Denmark); they discovered that the main species, Hg^{+2}, is of volcanic origin and may be used as indicator of volcanic activity during extreme climatic and biotic events. Similar studies are needed on a global basis to document the causes and consequences of extreme climatic and biotic events during the K-T boundary transition.

Ocean Acidification and Its Biotic Effects

Large-scale volcanism can severely perturb the carbon cycle due to the increased CO_2 emissions into the atmosphere. Loading of pCO_2 at a rate faster than the buffering time/capacity of the ocean (~1000 yr; Zeebe, 2012) can significantly affect seawater carbonate chemistry. Equilibration at the atmosphere-ocean interface would result in lowering of the CO_3^{2-} ion concentration and/or lowering of the surface ocean pH (Kump et al., 2009). Acidification would therefore lead to a calcification crisis for the carbonate-secreting planktons such as coccolithophores, foraminifera, and pteropods. The removal of huge volumes of volcanic SO_2 as acid rain would also lead to short-term lowering of surface ocean pH and cause severe biotic stress. Several faunal turnovers and mass extinction events that affected marine calcifiers in geological history may have involved ocean acidification events, including ocean anoxic events of the Paleozoic and the Paleocene-Eocene thermal maximum (see review in Hönisch et al., 2012). Dwarfism, malformed individuals, and R-strategist–dominated assemblages are recorded in calcareous nannoplankton during oceanic anoxic event 1a (OAE 1a), likely linked with stepwise accumulation of CO_2 in the ocean and progressive acidification (Erba et al., 2010).

In the past ~300 yr, the pH of the ocean has dropped by 0.1 units, and a further drop of 0.7 units is expected in the next ~300 yr due to anthropogenic CO_2 emissions. At this rate, models predict the southern oceans to become undersaturated with respect to aragonite in the next 50 yr and with respect to calcite in the next 100 yr (Orr et al., 2005; Zeebe et al., 2008). Experiments show that shell dissolution in live pteropods begins in less than 48 h on exposure to undersaturated waters (Fabry et al., 2008; Doney et al., 2009). Calcite-precipitating organisms are likely to suffer similar test dissolution on further acidification. Laboratory culture experiments confirm a decrease in the shell mass of planktic foraminifera with a decrease in [CO_3^{2-}] of ambient water (Spero et al., 1997; Bijma et al., 1999). Acidification appears to have resulted in a 30%–35% reduction in calcification in modern *Globigerina bulloides* from the Southern Ocean as compared to Holocene specimens (Moy et al., 2009). Modern benthic foraminifera in sediments associated with shallow volcanic CO_2 seeps in Papua New Guinea show a decline in abundance and diversity correlative with decreasing pH (with complete absence in pH <7.9, >700 μatm pCO_2; Uthicke et al., 2013).

Deccan Volcanism and Ocean Acidification

Deccan volcanism phase 2 during the late Maastrichtian occurred as a series of at least 30 major eruptive events. The estimated CO_2 emission rate for each single eruptive event is up to 20 Gt/yr (assuming a maximum duration of ~10 yr for each event; Chenet et al., 2009; Courtillot and Fluteau, this volume). This rate is comparable with the magnitude of anthropogenic CO_2 loading (~30 Gt/yr) since the advent of the industrial revolution (Forster et al., 2007). A single Deccan eruptive event, or meteorite impact, of geologically short duration could result in ocean acidification that persisted for no more than 1000 yr (Gibbs et al., 2010), which may not be resolvable in the sedimentary record. However, the rapid succession (months, years, decades to 100,000 yr; Courtillot and Fluteau, this volume) of major Deccan eruptive events likely changed the seawater chemistry of the ocean, resulting in ocean acidification within a few hundred years of the onset of volcanism (analogous to the present-day anthropogenic situation of 300–600 yr) and may have lasted for 10,000–100,000 yr (the time scale of restoration of pre-perturbation marine [CO_3^{2-}] by continental weathering processes; Archer, 2005; Hönisch et al., 2012). At this time scale, the effects of ocean acidification would have persisted long enough to be resolved in the sediment record. The episodic nature of Deccan eruptions leading to ocean acidification along with changes in water mass stratification caused by rapid global warming and cooling may explain the severe stress conditions for marine calcifiers near the end of the Maastrichtian.

Although this is a compelling hypothesis, acidification as a kill mechanism in the mass extinction of planktic foraminifera still requires rigorous evaluation. The intervals that record faunal stress must be tested for paleo-pH or [CO_3^{2-}] changes using proxies such as $\delta^{11}B$, B/Ca, and Zn/Ca (Yu and Elderfield, 2007; Hönisch et al., 2012). Dissolution-based proxies such as $CaCO_3$ %

and foraminiferal shell weight may also be used as supporting evidence in sections that have not been significantly affected by postdepositional dissolution and recrystallization.

DECCAN VOLCANISM AND DELAYED RECOVERY AFTER THE MASS EXTINCTION

The delayed recovery in marine biota in the aftermath of the K-T boundary mass extinction has remained an enigma ever since the beginning of the K-T boundary debate (Hsü and McKenzie, 1985; Keller, 1988a, 1989a; Magaritz et al., 1992; review in Keller and Abramovich, 2009). Magaritz et al. (1992) first identified a major δ^{13}C anomaly associated with a black clay layer in the early Danian section in the Negev, Israel, and Keller and Benjamini (1991) documented very high abundances of *G. cretacea*, identifying this event as a major high-stress environment similar to the immediate aftermath of the K-T boundary mass extinction. More recently, Quillévéré et al. (2008) observed negative δ^{18}O and δ^{13}C anomalies in the North Atlantic ODP Site 1049C, and DSDP Sites 527 and 528, in zone P1a of Berggren et al. (1995), which corresponds to zone P1b of Keller et al. (1995; Fig. 8), and labeled this the hyperthermal Dan-C2 event. Coccioni et al. (2010) linked this warming to the last phase of Deccan volcanism, which began near the base of chron C29n coincident with the zone P1a-P1b boundary (Chenet et al., 2007, 2008, 2009; Keller et al., 2008, 2011a).

Keller et al. (2011a, 2012) documented zones P1a, P1b, and P1c assemblages in sediments below, between, and above the megaflows of Deccan phase 3 in nine deep wells of the Krishna-Godavari Basin. The early Danian planktic foraminiferal turnover associated with Deccan volcanism records the same low diversity, small species morphologies, and sequence of appearances/disappearances as observed in zones P1a and P1b worldwide. Biotic recovery to larger size and higher diversity followed in zone P1c after Deccan phase 3 ended. This study firmly links the early Danian high-stress environment and delayed recovery to the last phase 3 of Deccan volcanism. High-stress environments in zone P1b are evident by blooms of the opportunistic species *Guembelitria* and/or *Gl. daubjergensis* from India to the eastern Tethys (Israel and Egypt) and Texas (Figs. 16 and 17).

Interestingly, there are no extinctions associated with the Danian perturbations. Several factors can explain the differing responses between Deccan phase 2 and phase 3: (1) phase 3 volcanic eruptions were not as frequent or extreme as in phase 2 and therefore permitted ecosystem recovery between eruptions. (2) Climate changes associated with phase 3 were less extreme compared with phase 2 during the latest Maastrichtian, when temperatures on land rose by 5–8 °C and temperatures in the deep sea rose by 3–4 °C (Li and Keller, 1998b, 1998c; Nordt et al., 2003; Wilf et al., 2003). (3) Deccan phase 3 accounts for 14% of the total Deccan eruption volume as compared with 80% for phase 2. (4) The less catastrophic biotic response to phase 3 volcanism is at least partly related to faunal assemblages that evolved during post–K-T boundary high-stress environments and

therefore were better adapted with a wider range of tolerance than the highly specialized Maastrichtian species.

CONCLUSIONS AND FUTURE WORK

Until a few years ago, the K-T boundary mass extinction was commonly attributed to the Chicxulub impact as the sole cause, and the long-term pre- and postextinction climatic, environmental, and faunal changes were either denied as nonexisting or ignored as unrelated to the mass extinction (see Schulte et al., 2010). Today, it is generally recognized that large igneous province volcanism played a major role in four out of five mass extinctions, including that at the K-T boundary (Bond and Wignall, this volume; Courtillot and Fluteau, this volume; Keller, this volume). Deccan volcanism is the only large igneous province event where a mass extinction has been documented in sediments between major basalt flows, providing an excellent case study for evaluation of the immediate effects of volcanic eruptions on marine life. This review summarizes the global climatic and faunal changes associated with the main Deccan phase 2 that led to the K-T boundary mass extinction and the last phase 3 that delayed recovery in the early Danian for at least 500 k.y. (Fig. 18). The initial Deccan phase 1, which accounts for ~6% of the total basalt eruptions, can also be recognized by *Guembelitria* blooms in India and Texas in zone CF4. However, there are little data available on this time interval to date.

There are still many challenges in working out the details of the faunal and climatic records globally and correlating these to Deccan volcanism. The major hurdle is the incomplete record in most localities, with hiatuses at the K-T boundary, within zone P1a, and at the P1a-P1b boundary. These short hiatuses are generally not recognized by routine biostratigraphic analysis based solely on the presence or absence of the index species, which frequently leads to erroneous conclusions that the record is complete when in fact just a small fraction of a biozone is preserved. High-resolution quantitative faunal analysis is necessary to determine the completeness of the sedimentation records, though such studies are often not done because they are very labor intensive.

Another challenge is the accurate evaluation of the age and tempo of the individual pulsed eruptions and megaflows, which requires chronologic dating using zircons for maximum age resolution. Equally important are accurate age estimates for the duration of quiescent intervals between eruptive events; it is possible that good age estimates can be obtained from red bole horizons between Deccan flows and from intertrappean marine sediments.

Multidisciplinary studies and use of a wide variety of geochemical proxies are required to understand the deleterious effects of Deccan volcanism on climate, the environment, and marine biota, with particular emphasis on potential stress and kill mechanisms, such as surface ocean acidification, marine calcification crisis, increased continental weathering, and nutrient and productivity changes.

Better atmospheric and oceanic global climate models for the late Maastrichtian–early Danian based on geochemical,
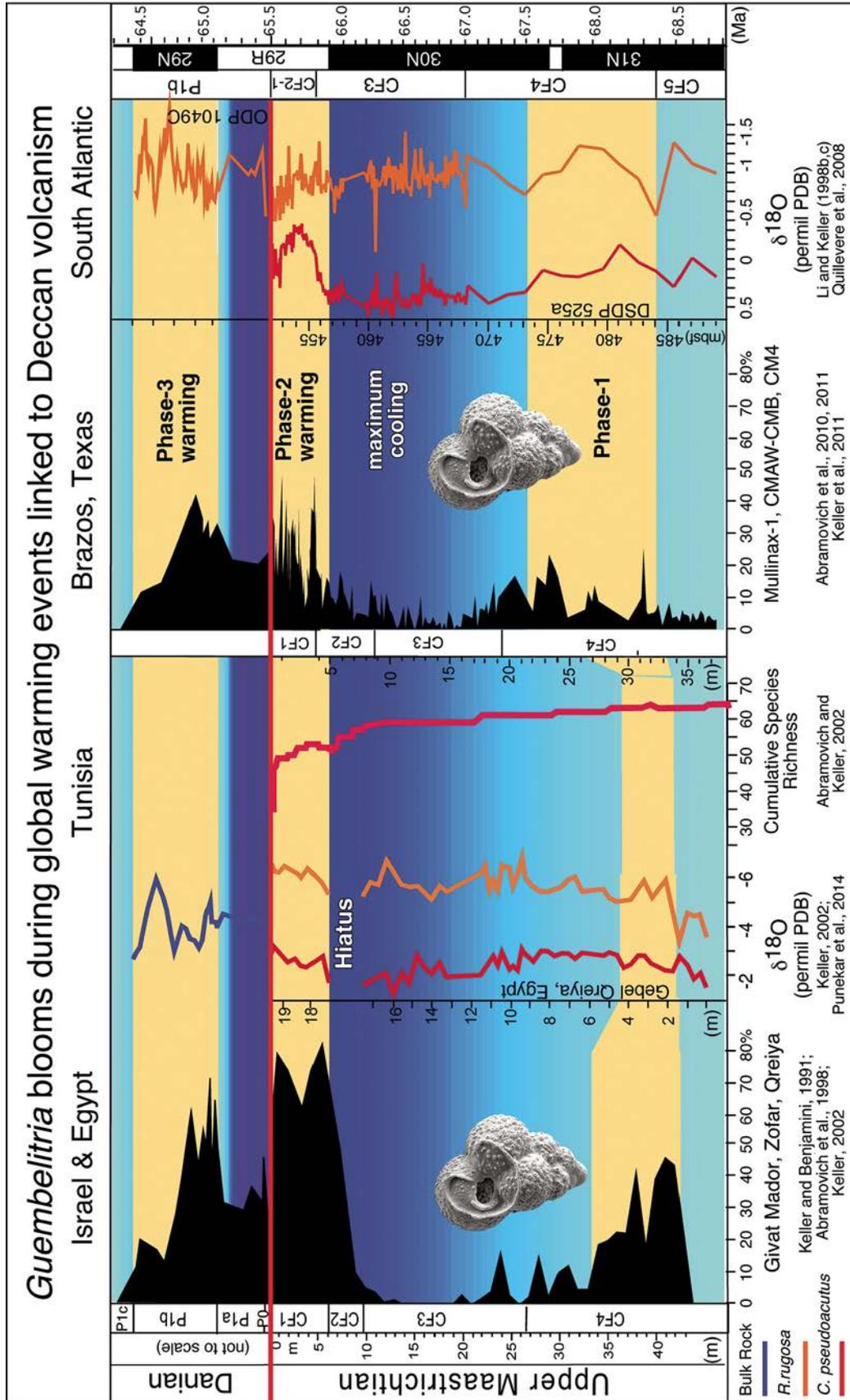
Figure 18. Global warming and faunal stress events during the late Maastrichtian and early Danian correlate with the three phases of Deccan volcanism. DSDP—Deep Sea Drilling Project; ODP—Ocean Drilling Program; PDB—Peedee belemnite; *R. rugosa*—*Rugoglobigerina rugosa*; *C. pseudoacuta*—*Cibicidoides pseudoacuta*.

paleoclimatic, and faunal records could improve our understanding of the runaway effects that likely caused the mass extinction.

ACKNOWLEDGMENTS

REFERENCES CITED

Abramovich, S., and Keller, G., 2002, High stress late Maastrichtian paleoenvironment: Inference from planktonic foraminifera in Tunisia: Palaeogeography, Palaeoclimatology, Palaeoecology, v. 178, p. 145–164, doi:10.1016/S0031-0182(01)00394-7.

Abramovich, S., and Keller, G., 2003, Planktonic foraminiferal response to the latest Maastrichtian abrupt warm event: A case study from South Atlantic DSDP Site 525A: Marine Micropaleontology, v. 48, no. 3–4, p. 225–249, doi:10.1016/S0377-8398(03)00021-5.

Abramovich, S., Almongi-Labin, A., and Benjamini, C., 1998, Decline of the Maastrichtian pelagic ecosystem based on planktic foraminifera assemblage changes: Implication for the terminal Cretaceous faunal crisis: Geology, v. 26, p. 63–66, doi:10.1130/0091-7613(1998)026<0063:DOTMPE>2.3.CO;2.

Abramovich, S., Keller, G., Adatte, T., Stinnesbeck, W., and Hottinger, L., 2002, Age and paleoenvironment of the Maastrichtian to Paleocene of the Mahajanga Basin, Madagascar : A multidisciplinary approach: Marine Micropaleontology, v. 47, p. 17–70, doi:10.1016/S0377-8398(02)00094-4.

Abramovich, S., Keller, G., Stüeben, D., and Berner, Z., 2003, Characterization of late Campanian and Maastrichtian planktonic foraminiferal depth habitats and vital activities based on stable isotopes: Palaeogeography, Palaeoclimatology, Palaeoecology, v. 202, no. 1–2, p. 1–29, doi:10.1016/S0031-0182(03)00572-8.

Abramovich, S., Yovel-Corem, S., Almogi-Labin, A., and Benjamini, C., 2010, Global climate change and planktic formaminiferal response in the Maastrichtian: Paleoceanography, v. 25, p. PA2201, doi:10.1029/2009PA001843.

Abramovich, S., Keller, G., Berner, Z., Cymbalista, M., and Rak, C., 2011, Maastrichtian planktic foraminiferal biostratigraphy and paleoenvironment of Brazos River, Falls County, Texas, *in* Keller, G., and Adatte, T., eds., The End-Cretaceous Mass Extinction and the Chicxulub Impact in Texas: Society for Sedimentary Geology (SEPM) Special Publication 100, p. 123–156.

Adatte, T., Keller, G., and Baum, G., 2011, Age and origin of the Chicxulub impact and sandstone complex, Brazos River, Texas: Evidence from lithostratigraphy and sedimentology, *in* Keller, G., and Adatte, T., eds., The End-Cretaceous Mass Extinction and the Chicxulub Impact in Texas: Society for Sedimentary Geology (SEPM) Special Publication 100, p. 43–80.

Archer, D., 2005, Fate of fossil fuel CO_2 in geological time: Journal of Geophysical Research, v. 111, C09S05, doi:10.1029/2004JC002625.

Arenillas, I., Arz, J.A., Molina, E., and Dupuis, C., 2000, The Cretaceous/Tertiary boundary at Ain Settara, Tunisia: Sudden catastrophic mass extinction in planktic foraminifera: Journal of Foraminiferal Research, v. 30, p. 202–218, doi:10.2113/0300202.

Arenillas, I., Arz, J.A., Grajales-Nishimura, J.M., Murillo-Muneton, G., Alvarez, W., Camargo-Zanguera, A., Molina, E., and Rosales-Dominguez, C., 2006, Chicxulub impact event is Cretaceous/Paleogene boundary in age: New micropaleontological evidence: Earth and Planetary Science Letters, v. 249, p. 241–257, doi:10.1016/j.epsl.2006.07.020.

Barrera, E., and Keller, G., 1990, Foraminiferal stable isotope evidence for gradual decrease of marine productivity and Cretaceous species survivorship in the earliest Danian: Paleoceanography, v. 5, p. 867–890, doi:10.1029/PA005i006p00867.

Begon, M., Mortimer, M., and Thompson, D.J., 1996, Population Ecology: A Unified Study of Plants and Animals: Cambridge, UK, Blackwell, 247 p.

Begon, M., Harper, J.L., and Townsend, C.R., 1998, Ecology: Individuals, Populations and Communities: Boston, Blackwell Science, 1068 p.

Berggren, W.A., Kent, D.V., Swisher, C.C., III, and Aubry, M.-P., 1995, A revised Cenozoic geochronology and chronostratigraphy, *in* Berggren, W.A., Kent, D.V., Aubry, M.-P., and Hardenbol, J., eds., Geochronology, Time Scales and Global Stratigraphic Correlation: Society for Sedimentary Geology (SEPM) Special Publication 54, p. 129–212.

Bijma, J., Spero, H.J., and Lea, D.W., 1999, Reassessing foraminiferal stable isotope geochemistry: Impact of the oceanic carbonate system (experimental results), *in* Fischer, G., and Wefer, G., eds., Use of Proxies in Paleoceanography: Examples from the South Atlantic: Berlin, Springer, p. 489–512.

Bond, D.P.G., and Wignall, P.B., 2014, this volume, Large igneous provinces and mass extinctions: An update, *in* Keller, G., and Kerr, A.C., eds., Volcanism, Impacts, and Mass Extinctions: Causes and Effects: Geological Society of America Special Paper 505, doi:10.1130/2014.2505(02).

Brayshay, M., and Grattan, J., 1999, Environmental and social responses in Europe to the 1783 eruption of the Laki fissure volcano in Iceland: A consideration of contemporary documentary evidence, *in* Firth, C.R., and McGuire, W.J., eds., Volcanoes in the Quaternary: Geological Society of London Special Publication 161, p. 173–188.

Buzas, M.A., and Gibson, T.G., 1969, Species diversity: Benthonic foraminifera in the western North Atlantic: Science, v. 163, p. 72–75, doi:10.1126/science.163.3862.72.

Cande, S., and Kent, D.V., 1995, Revised calibration of the geomagnetic polarity timescale for the Late Cretaceous and Cenozoic: Journal of Geophysical Research, v. 100, p. 6093–6095, doi:10.1029/94JB03098.

Canudo, J.I., Keller, G., and Molina, E., 1991, Cretaceous/Tertiary boundary extinction pattern and faunal turnover at Agost and Caravaca, SE Spain: Marine Micropaleontology, v. 17, p. 319–341, doi:10.1016/0377-8398(91)90019-3.

Chenet, A.-L., Quidelleur, X., Fluteau, F., Courtillot, V., and Bajpai, S., 2007, $^{40}K/^{40}Ar$ dating of the main Deccan large igneous province: Further evidence of Cretaceous-Tertiary boundary age and short duration: Earth and Planetary Science Letters, v. 263, p. 1–15, doi:10.1016/j.epsl.2007.07.011.

Chenet, A.-L., Fluteau, F., Courtillot, V., Gerard, M., and Subbarao, K.V., 2008, Determination of rapid Deccan eruptions across the Cretaceous-Tertiary boundary using paleomagnetic secular variation: Results from a 1200-m-thick section in the Mahabaleshwar: Journal of Geophysical Research, v. 113, B04101, doi:10.1029/2006JB004635.

Chenet, A.-L., Courtillot, V., Fluteau, F., Gerard, M., Quidelleur, X., Khadri, S.F.R., Subbarao, K.V., and Thordarson, T., 2009, Determination of rapid Deccan eruptions across the Cretaceous-Tertiary boundary using paleomagnetic secular variation: 2. Constraints from analysis of eight new sections and synthesis for a 3500-m-thick composite section: Journal of Geophysical Research, v. 114, B06103, doi:10.1029/2008JB005644.

Coccioni, R., and Luciani, V., 2006, *Guembelitria irregularis* bloom at the K-T boundary: Morphological abnormalities induced by impact-related extreme environmental stress?, *in* Cockell, C., Koeberl, C., and Gilmour, I., eds., Biological Processes Associated with Impact Events: Impact Studies: Berlin, Springer, p. 179–196.

Coccioni, R., Frontalini, F., Bancalà, G., Fornaciari, E., Jovane, L., and Sprovieri, M., 2010, The Dan-C2 hyperthermal event at Gubbio (Italy): Global implications, environmental effects, and cause(s): Earth and Planetary Science Letters, v. 297, p. 298–305, doi:10.1016/j.epsl.2010.06.031.

Courtillot, V., and Fluteau, F., 2014, this volume, A review of the embedded time scales of flood basalt volcanism with special emphasis on dramatically short magmatic pulses, *in* Keller, G., and Kerr, A.C., eds., Volcanism, Impacts, and Mass Extinctions: Causes and Effects: Geological Society of America Special Paper 505, doi:10.1130/2014.2505(15).

D'Hondt, S., and Keller, G., 1991, Some patterns of planktic foraminiferal assemblage turnover at the Cretaceous-Tertiary boundary: Marine Micropaleontology, v. 17, p. 77–118, doi:10.1016/0377-8398(91)90024-Z.

Doney, S.C., Fabry, V.J., Feely, R.A., and Kleypas, J.A., 2009, Ocean acidification: The other CO_2 problem: Annual Review of Marine Science, v. 1, p. 169–192, doi:10.1146/annurev.marine.010908.163834.

Erba, E., Bottini, C., Weissert, H.J., and Keller, C.E., 2010, Calcareous nannoplankton response to surface-water acidification around oceanic

anoxic event 1a: Science, v. 329, no. 5990, p. 428–432, doi:10.1126/science.1188886.

Fabry, V.J., Seibel, B.A., Feely, R.A., and Orr, J.C., 2008, Impacts of ocean acidification on marine fauna and ecosystem processes: ICES Journal of Marine Science: Journal du Conseil, v. 65, no. 3, p. 414–432, doi:10.1093/icesjms/fsn048.

Font, E., Nedelec, A., Ellwood, B.B., Mirao, J., and Silva, P.F., 2011, A new sedimentary benchmark for the Deccan Traps volcanism?: Geophysical Research Letters, v. 38, L24309, doi:10.1029/2011GL049824.

Font, E., Fabre, S., Nédélec, A., Adatte, T., Keller, G., Veiga-Pires, C., Ponte, J., Mirão, J., Khozyem, H., and Spangenberg, J., 2014, this volume, Atmospheric halogen and acid rains during the main phase of Deccan eruptions: Magnetic and mineral evidence, *in* Keller, G., and Kerr, A.C., eds., Volcanism, Impacts and Mass Extinctions: Causes and Effects: Geological Society of America Special Paper 505, doi:10.1130/2014.2505(18).

Forster, P., Ramaswamy, V., Artaxo, P., Berntsen, T., Betts, R., Fahey, D.W., Haywood, J., Lean, J., Lowe, D.C., Myhre, G., Nganga, J., Prinn, R., Raga, G., Schultz, M., and Van Dorland, R., 2007, Changes in atmospheric constituents and in radiative forcing, *in* Solomon., S., et al., eds., Climate Change 2007: The Physical Science Basis. Contribution of Working Group I to the Fourth Assessment Report of the Intergovernmental Panel on Climate Change: Cambridge, UK, Cambridge University Press, p. 129–234.

Ganino, C., and Arndt, N.T., 2009, Climate changes caused by degassing of sediments during the emplacement of large igneous provinces: Geology, v. 37, p. 323–326, doi:10.1130/G25325A.1.

Gertsch, B., Keller, G., Adatte, T., Garg, R., Prasad, V., Fleitmann, D., and Berner, Z., 2011, Environmental effects of Deccan volcanism across the Cretaceous-Tertiary transition in Meghalaya, India: Earth and Planetary Science Letters, v. 310, p. 272–285, doi:10.1016/j.epsl.2011.08.015.

Gibbs, S.J., Stoll, H.M., Brown, P.R., and Bralower, T.J., 2010, Ocean acidification and surface water carbonate production across the Paleocene-Eocene thermal maximum: Earth and Planetary Science Letters, v. 295, p. 583–592, doi:10.1016/j.epsl.2010.04.044.

Gilmour, I., Gilmour, M., Jolley, D.W., Kelley, S.P., Kemp, D.B., Daly, R.J., and Watson, J.S., 2013, A high-resolution nonmarine record of an early Danian hyperthermal event, Boltysh Crater, Ukraine: Geology, v. 41, p. 783–786, doi:10.1130/G34292.1.

Ginsburg, R.N., 1997a, An attempt to resolve the controversy over the end-Cretaceous extinction of planktic foraminifera at El Kef, Tunisia, using a blind test; introduction; background and procedures: Marine Micropaleontology, v. 29, no. 2, p. 67–68, doi:10.1016/S0377-8398(96)00038-2.

Ginsburg, R.N., 1997b, Not so blind El Kef test: Marine Micropaleontology, v. 32, no. 3–4, p. 399, doi:10.1016/S0377-8398(97)89276-6.

Ginsburg, R.N., 1997c, Perspectives on the blind test: Marine Micropaleontology, v. 29, no. 2, p. 101–103, doi:10.1016/S0377-8398(96)00046-1.

Gradstein, F., Ogg, J., and Smith, A., 2004, A Geologic Time Scale: Cambridge, UK, Cambridge University Press, 598 p.

Gradstein, F.M., Ogg, G., and Schmitz, M., 2012, The Geologic Time Scale 2-Volume Set: Amsterdam, Elsevier, 912 p.

Grattan, J., Durand, M., and Taylor, S., 2003, Illness and elevated human mortality in Europe coincident with the Laki fissure eruption, *in* Oppenheimer C., Pyle, D.M., and Barclay J., eds., Volcanic Degassing: Geological Society of London Special Publication 213, p. 401–414.

Hönisch, B., Ridgwell, A., Schmidt, D.N., Thomas, E., Gibbs, S.J., Sluijs, A., Zeebe, R., Kump, L., Martindale, R.C., Greene, S.E., Kiessling, G., Ries, J., Zachos, J.C., Royer, D.L., Barker, S., Marchitto, T.M., Jr., Moyer, R., Pelejero, C., Ziveri1, P., Foster, G.L., and Williams, B., 2012, The geological record of ocean acidification: Science, v. 335, no. 6072, p. 1058–1063, doi:10.1126/science.1208277.

Hsü, K.J., and McKenzie, J.A., 1985, A "strangelove" ocean in earliest Tertiary, *in* Sundquist, E.T., and Broecker, W., eds., The Carbon Cycle and Atmospheric CO$_2$: Natural Variations Archean to Present: American Geophysical Union Geophysical Monograph 32, p. 487–492.

Jay, A.E., and Widdowson, M., 2008, Stratigraphy, structure and volcanology of the south-east Deccan continental flood basalt province: Implications for eruptive extent and volumes: Journal of the Geological Society of London, v. 165, p. 177–188, doi:10.1144/0016-76492006-062.

Keller, G., 1988a, Extinction, survivorship and evolution of planktic foraminifers across the Cretaceous/Tertiary boundary at El Kef, Tunisia: Marine Micropaleontology, v. 13, p. 239–263, doi:10.1016/0377-8398(88)90005-9.

Keller, G., 1988b, Biotic turnover in benthic foraminifera across the Cretaceous-Tertiary boundary at El Kef, Tunisia: Palaeogeography, Palaeoclimatology, Palaeoecology, v. 66, p. 153–171, doi:10.1016/0031-0182(88)90198-8.

Keller, G., 1989a, Extended period of extinctions across the K/T boundary in planktic foraminifera of continental shelf sections: Implications for impact and volcanism theories: Geological Society of America Bulletin, v. 101, p. 1408–1419, doi:10.1130/0016-7606(1989)101<1408:EPOEAT>2.3.CO;2.

Keller, G., 1989b, Extended K/T boundary extinctions and delayed populational change in planktic foraminiferal faunas from Brazos River, Texas: Paleoceanography, v. 4, no. 3, p. 287–332, doi:10.1029/PA004i003p00287.

Keller, G., 1993, The Cretaceous-Tertiary boundary transition in the Antarctic Ocean and its global implications: Marine Micropaleontology, v. 21, p. 1–45, doi:10.1016/0377-8398(93)90010-U.

Keller, G., 2001, The end-Cretaceous mass extinction in the marine realm: Year 2000 assessment: Planetary and Space Science, v. 49, no. 8, p. 817–830, doi:10.1016/S0032-0633(01)00032-0.

Keller, G., 2002, *Guembelitria*-dominated late Maastrichtian planktic foraminiferal assemblages mimic early Danian in central Egypt: Marine Micropaleontology, v. 47, p. 71–99, doi:10.1016/S0377-8398(02)00116-0.

Keller, G., 2003, Biotic effects of impacts and volcanism: Earth and Planetary Science Letters, v. 215, no. 1–2, p. 249–264, doi:10.1016/S0012-821X(03)00390-X.

Keller, G., 2004, Low-diversity, late Maastrichtian and early Danian planktic foraminiferal assemblages of the eastern Tethys: Journal of Foraminiferal Research, v. 34, no. 1, p. 49–73, doi:10.2113/0340049.

Keller, G., 2005, Biotic effects of late Maastrichtian mantle plume volcanism: Implications for impacts and mass extinctions: Lithos, v. 79, no. 3–4, p. 317–341, doi:10.1016/j.lithos.2004.09.005.

Keller, G., 2008a, Cretaceous climate, volcanism, impacts and biotic effects: Cretaceous Research, v. 29, no. 5–6, p. 754–771, doi:10.1016/j.cretres.2008.05.030.

Keller, G., 2008b, Impact stratigraphy: Old principle, new reality, *in* Evans, K.R., Horton, J.W., and King, D.T., eds., The Sedimentary Record of Meteorite Impacts: Geological Society of America Special Paper 437, p. 147–178.

Keller, G., 2011, Cretaceous-Tertiary mass extinction in marginal and open marine environments: Texas, U.S.A., and Tunisia, *in* Keller, G., and Adatte, T., eds., The End-Cretaceous Mass Extinction and the Chicxulub Impact in Texas: Society for Sedimentary Geology (SEPM) Special Publication 100, p. 197–226.

Keller, G., 2014, this volume, Deccan volcanism, the Chicxulub impact, and the end-Cretaceous mass extinction: Coincidence? Cause and effect?, *in* Keller, G., and Kerr, A.C., eds., Volcanism, Impacts, and Mass Extinctions: Causes and Effects: Geological Society of America Special Paper 505, doi:10.1130/2014.2505(03).

Keller, G., and Abramovich, S., 2009, Lilliput effect in late Maastrichtian planktic foraminifera: Response to environmental stress: Palaeogeography, Palaeoclimatology, Palaeoecology, v. 284, p. 47–62, doi:10.1016/j.palaeo.2009.08.029.

Keller, G., and Benjamini, C., 1991, Paleoenvironment of the eastern Tethys in the early Danian: Palaios, v. 6, p. 439–464, doi:10.2307/3514984.

Keller, G., and Pardo, A., 2004, Disaster opportunists Guembelitrinidae—Index for environmental catastrophes: Marine Micropaleontology, v. 53, p. 83–116, doi:10.1016/j.marmicro.2004.04.012.

Keller, G., Barrera, E., Schmitz, B., and Matsson, E., 1993, Gradual mass extinction, species survivorship, and long term environmental changes across the Cretaceous-Tertiary boundary in high latitudes: Geological Society of America Bulletin, v. 105, no. 8, p. 979–997, doi:10.1130/0016-7606(1993)105<0979:GMESSA>2.3.CO;2.

Keller, G., Stinnesbeck, W., and Lopez-Oliva, J. G, 1994, Age, deposition and biotic effects of the Cretaceous/Tertiary boundary event at Mimbral, NE Mexico: Palaios, v. 9, no. 2, p. 144–157.

Keller, G., Li, L., and MacLeod, N., 1996, The Cretaceous/Tertiary boundary stratotype section at El Kef, Tunisia: How catastrophic was the mass extinction?: Palaeogeography, Palaeoclimatology, Palaeoecology, v. 119, p. 221–254, doi:10.1016/0031-0182(95)00009-7.

Keller, G., Adatte, T., Stinnesbeck, W., Luciani, V., Karoui, N., and Zaghbib-Turki, D., 2002a, Paleoecology of the Cretaceous-Tertiary mass extinction in planktic foraminifera: Palaeogeography, Palaeoclimatology, Palaeoecology, v. 178, p. 257–297, doi:10.1016/S0031-0182(01)00399-6.

Effects of Deccan volcanism on paleoenvironment and planktic foraminifera: A global survey

Keller, G., Adatte, T., Burns, S.J., and Tantawy, A.A., 2002b, High-stress paleoenvironment during the late Maastrichtian to early Paleocene in central Egypt: Palaeogeography, Palaeoclimatology, Palaeoecology, v. 187, no. 1, p. 35–60, doi:10.1016/S0031-0182(02)00504-7.

Keller, G., Adatte, T., Tantawy, A.A., Berner, Z., Stinnesbeck, W., Stueben, D., and Leanza, H.A., 2007, High stress late Maastrichtian–early Danian palaeoenvironment in the Neuquén Basin, Argentina: Cretaceous Research, v. 28, no. 6, p. 939–960, doi:10.1016/j.cretres.2007.01.006.

Keller, G., Adatte, T., Gardin, S., Bartolini, A., and Bajpai, S., 2008, Main Deccan volcanism phase ends near the K-T boundary: Evidence from the Krishna-Godavari Basin, SE India: Earth and Planetary Science Letters, v. 268, p. 293–311, doi:10.1016/j.epsl.2008.01.015.

Keller, G., Khosla, S.C., Sharma, R., Khosla, A., Bajpai, S., and Adatte, T., 2009, Early Danian planktic foraminifera from Cretaceous-Tertiary intertrappean beds at Jhilmili, Chhindwara District, Madhya Pradesh, India: Journal of Foraminiferal Research, v. 39, no. 1, p. 40–55, doi:10.2113/gsjfr.39.1.40.

Keller, G., Bhowmick, P.K., Upadhyay, H., Dave, A., Reddy, A.N., Jaiprakash, B.C., and Adatte, T., 2011a, Deccan volcanism linked to the Cretaceous-Tertiary boundary (KTB) mass extinction: New evidence from ONGC wells in the Krishna-Godavari Basin, India: Journal of the Geological Society of India, v. 78, p. 399–428, doi:10.1007/s12594-011-0107-3.

Keller, G., Abramovich, S., Adatte, T., and Berner, Z., 2011b, Biostratigraphy, age of the Chicxulub impact, and depositional environment of the Brazos River KTB sequences, *in* Keller, G., and Adatte, T., eds., The End-Cretaceous Mass Extinction and the Chicxulub Impact in Texas: Society for Sedimentary Geology (SEPM) Special Publication 100, p. 81–122.

Keller, G., Adatte, T., Bhowmick, P.K., Upadhyay, H., Dave, A., Reddy, A.N., and Jaiprakash, B.C., 2012, Nature and timing of extinctions in Cretaceous-Tertiary planktic foraminifera preserved in Deccan intertrappean sediments of the Krishna-Godavari Basin, India: Earth and Planetary Science Letters, v. 341–344, p. 211–221, doi:10.1016/j.epsl.2012.06.021.

Keller, G., Khozyem, H.M., Adatte, T., Malarkodi, N., Spangenberg, J.E., and Stinnesbeck, W., 2013, Chicxulub impact spherules in the North Atlantic and Caribbean: Age constraints and Cretaceous-Tertiary boundary hiatus: Geological Magazine, v. 150, no. 5, p. 885–907, doi:10.1017/S0016756812001069.

Kucera, M., and Malmgren, B.A., 1998, Terminal Cretaceous warming event in the mid-latitude South Atlantic Ocean: Evidence from poleward migration of *Contusotruncana contusa* (planktonic foraminifera) morphotypes: Palaeogeography, Palaeoclimatology, Palaeoecology, v. 138, p. 1–15, doi:10.1016/S0031-0182(97)00124-7.

Kump, L., Bralower, T., and Ridgwell, A., 2009, Ocean acidification in deep time: Oceanography, v. 22, no. 4, p. 94–107.

Lamolda, M.A., Melinte, M.C., and Kaiho, K., 2005, Nannofloral extinction and survivors across the K/T boundary at Caravaca, southeastern Spain: Palaeogeography, Palaeoclimatology, Palaeoecology, v. 224, p. 27–52, doi:10.1016/j.palaeo.2005.03.030.

Li, L., and Keller, G., 1998a, Maastrichtian climate, productivity and faunal turnovers in planktic foraminifera of South Atlantic DSDP Sites 525A and 21: Marine Micropaleontology, v. 33, no. 1–2, p. 55–86, doi:10.1016/S0377-8398(97)00027-3.

Li, L., and Keller, G., 1998b, Abrupt deep-sea warming at the end of the Cretaceous: Geology, v. 26, p. 995–998, doi:10.1130/0091-7613(1998)026<0995:ADSWAT>2.3.CO;2.

Li, L., and Keller, G., 1998c, Diversification and extinction in Campanian-Maastrichtian planktic foraminifera of northwestern Tunisia: Eclogae Geologica Helvetiae, v. 91, p. 75–102.

Lipps, J.H., 1997, The Cretaceous-Tertiary boundary; the El Kef blind test: Marine Micropaleontology, v. 29, no. 2, p. 65–66, doi:10.1016/S0377-8398(96)00037-0.

Luciani, V., 1997, Planktonic foraminiferal turnover across the Cretaceous-Tertiary boundary in the Vajont valley (southern Alps, northern Italy): Cretaceous Research, v. 18, p. 799–821, doi:10.1006/cres.1997.0088.

Luciani, V., 2002, High resolution planktonic foraminiferal analysis from the Cretaceous/Tertiary boundary at Ain Settara (Tunisia): Evidence of an extended mass extinction: Palaeogeography, Palaeoclimatology, Palaeoecology, v. 178, no. 3, p. 299–319, doi:10.1016/S0031-0182(01)00400-X.

MacLeod, K.G., Huber, B.T., and Isaza-Londono, C., 2005, North Atlantic warming during global cooling at the end of the Cretaceous: Geology, v. 33, p. 437–440, doi:10.1130/G21466.1.

MacLeod, N., and Keller, G., 1991a, Hiatus distributions and mass extinctions at the Cretaceous/Tertiary boundary: Geology, v. 19, p. 497–501, doi:10.1130/0091-7613(1991)019<0497:HDAMEA>2.3.CO;2.

MacLeod, N., and Keller, G., 1991b, How complete are Cretaceous/Tertiary boundary sections? A chronostratigraphic estimate based on graphic correlation: Geological Society of America Bulletin, v. 103, p. 1439–1457, doi:10.1130/0016-7606(1991)103<1439:HCACTB>2.3.CO;2.

MacLeod, N., and Keller, G., 1994, Comparative biogeographic analysis of planktic foraminiferal survivorship across the Cretaceous/Tertiary (K/T) boundary: Paleobiology, v. 20, no. 2, p. 143–177.

MacLeod, N., Ortiz, N., Fefferman, N., Clyde, W., Schulter, C., and MacLean, J., 2000, Phenotypic response of foraminifera to episodes of global environmental change, *in* Culver, S.J., and Rawson, P., eds., Biotic Response to Global Environmental Change: The Last 145 Million Years: Cambridge, UK, Cambridge University Press, p. 51–78.

Magaritz, M., Benjamini, C., Keller, G., and Moshkovitz, S., 1992, Early diagenetic isotopic signal at the Cretaceous/Tertiary boundary, Israel: Palaeogeography, Palaeoclimatology, Palaeoecology, v. 91, no. 3, p. 291–304, doi:10.1016/0031-0182(92)90073-E.

Malarkodi, N., Keller, G., Fayazudeen, P.J., and Mallikarjuna, U.B., 2010, Foraminifera from the early Danian intertrappean beds in Rajahmundry Quarries, Andhra Pradesh, SE India: Journal of the Geological Society of India, v. 75, p. 851–863, doi:10.1007/s12594-010-0066-0.

Molina, E., Alegret, L., Arenillas, I., Arz, J., Gallala, N., Hardenbol, J., von Salis, K., Steurbaut, E., Vanhenberghe, N., and Zaghbib-Turki, D., 2006, The global boundary stratotype section and point for the base of the Danian Stage (Paleocene, Paleogene, "Tertiary," Cenozoic) at El Kef, Tunisia—Original definition and revision: Episodes, v. 29, no. 4, p. 263–273.

Moy, A.D., Howard, W.R., Bray, S.G., and Trull, T.W., 2009, Reduced calcification in modern Southern Ocean planktonic foraminifera: Nature Geoscience, v. 2, no. 4, p. 276–280, doi:10.1038/ngeo460.

Mussard, M., Le Hir, G., Fluteau, F., Lefebvre, V., and Goddéris, Y., 2014, this volume, Modeling the carbon-sulfate interplays in climate changes related to the emplacement of continental flood basalts, *in* Keller, G., and Kerr, A.C., eds., Volcanism, Impacts, and Mass Extinctions: Causes and Effects: Geological Society of America Special Paper 505, doi:10.1130/2014.2505(17).

Nordt, L., Atchley, S., and Dworkin, S., 2003, Terrestrial evidence for two greenhouse events in the latest Cretaceous: GSA Today, v. 13, no. 12, p. 4–9, doi:10.1130/1052-5173(2003)013<4:TEFTGE>2.0.CO;2.

Norris, R.D., Huber, B.T., and Self-Trail, B.T., 1999, Synchroneity of the KT oceanic mass extinction and meteorite impact: Blake Nose, western North Atlantic: Geology, v. 27, p. 419–422, doi:10.1130/0091-7613(1999)027<0419:SOTKTO>2.3.CO;2.

Olsson, R.K., Miller, K.G., Browning, J.V., Habib, D., and Sugarmann, P.J., 1997, Ejecta layer at the Cretaceous-Tertiary boundary, Bass River, New Jersey (Ocean Drilling Program Leg 174AX): Geology, v. 25, p. 759–762, doi:10.1130/0091-7613(1997)025<0759:ELATCT>2.3.CO;2.

Olsson, R.K., Hemleben, C., Berggren, W.A., and Huber, B.T., 1999, Atlas of Paleocene Planktonic Foraminifera: Smithsonian Contributions to Paleobiology 85: Washington, DC, Smithsonian Institution Press, 252 p.

Olsson, R.K., Wright, J.D., and Miller, K.G., 2001, Paleobiogeography of *Pseudotextularia elegans* during the latest Maastrichtian global warming event: Journal of Foraminiferal Research, v. 31, no. 3, p. 275–282, doi:10.2113/31.3.275.

Orr, J.C., Fabry, V.J., Aumont, O., Bopp, L., Doney, S.C., Feely, R.A., Gnanadesikan, A., Gruber, N., Ishida, A., Joos, F., Key, R.M., Lindsay, K., Maier-Reimer, E., Matear, R., Monfray, P., Mouchet, A., Najjar, R.G., Plattner, G-K., Rodgers, K.B., Sabine, C.L., Sarmiento, J.L., Schlitzer, R., Slater, R.D., Totterdell, I.J., Weirig, M-F., Yamanaka, Y., and Yool, A., 2005, Anthropogenic ocean acidification over the twenty-first century and its impact on calcifying organisms: Nature, v. 437, p. 681–686, doi:10.1038/nature04095.

Pardo, A., and Keller, G., 2008, Biotic effects of environmental catastrophes at the end of the Cretaceous: *Guembelitria* and *Heterohelix* blooms: Cretaceous Research, v. 29, no. 5–6, p. 1058–1073, doi:10.1016/j.cretres.2008.05.031.

Punekar, J., Keller, G., Khozyem, H.M., Hamming, C., Adatte, T., Tantawy, A.A., and Spangenberg, J., 2014, Late Maastrichtian–early Danian high-stress environments and delayed recovery linked to Deccan volcanism: Cretaceous Research, v. 49, p. 63–82.

Quillévéré, F., Norris, R.D., Kroon, D., and Wilson, P.A., 2008, Transient ocean warming and shifts in carbon reservoirs during the early Danian: Earth and Planetary Science Letters, v. 265, p. 600–615, doi:10.1016/j.epsl.2007.10.040.

Raja Rao, C.S., Sahasrabudhe, S.S., Deshmukh, S.S., and Raman, R., 1999, Distribution, structure and petrography of the Deccan Traps, India, *in* Subbarao, K.V., ed., Deccan Volcanic Province: Geological Society of India Memoir 43, p. 401–414.

Ravizza, G., and Peucker-Ehrenbrink, B., 2003, Chemostratigraphic evidence of Deccan volcanism from the marine osmium isotope record: Science, v. 302, p. 1392–1395, doi:10.1126/science.1089209.

Robinson, N., Ravizza, G., Coccioni, R., Peucker-Ehrenbrink, B., and Norris, R., 2009, A high-resolution marine 187Os/188Os record for the late Maastrichtian: Distinguishing the chemical fingerprints of Deccan volcanism and the KP impact event: Earth and Planetary Science Letters, v. 281, p. 159–168, doi:10.1016/j.epsl.2009.02.019.

Schulte, P., Alegret, L., Arenillas, I., Arz, J.A., Barton, P.J., Bown, P.R., Bralower, T.J., Christeson, G.L., Claeys, P., Cockell, C.S., Collins, G.S., Deutsch, A., Goldin, T.J., Goto, K., Grajales-Nishimura, J.M., Grieve, R.A.F., Gulick, S.P.S., Johnson, K.R., Kiessling, W., Koeberl, C., Kring, D.A., MacLeod, K.G., Matsui, T., Melosh, J., Montanari, A., Morgan, J.V., Neal, C.R., Nichols, D.J., Norris, R.D., Pierazzo, E., Ravizza, G., Rebolledo-Vieyra, M., Reimold, W.U., Robin, E., Salge, T., Speijer, R.P., Sweet, A.R., Urrutia-Fucugauchi, J., Vajda, V., Whalen, M.T., and Willumsen, P.S., 2010, The Chicxulub asteroid impact and mass extinction at the Cretaceous-Paleogene boundary: Science, v. 327, p. 1214–1218, doi:10.1126/science.1177265.

Self, S., Jay, A.E., Widdowson, M., and Keszthelyi, L.P., 2008, Correlation of the Deccan and Rajahmundry Trap lavas: Are these the longest and largest lava flows on Earth?: Journal of Volcanology and Geothermal Research, v. 172, p. 3–19, doi:10.1016/j.jvolgeores.2006.11.012.

Sial, A.N., Lacerda, L.D., Ferreira, V.P., Frei, R., Marquillas, R.A., Barbosa, J.A., Gaucher, C., Windmöller, C.C., and Pereira, N.S., 2013, Mercury as a proxy for volcanic activity during extreme environmental turnover: The Cretaceous–Paleogene transition: Palaeogeography, Palaeoclimatology, Palaeoecology, v. 387, p. 153–164.

Smit, J., 1982, Extinction and evolution of planktonic foraminifera after a major impact at the Cretaceous/Tertiary boundary, *in* Silver, L.T., and Schultz, P.H., eds., Geological Implications of Impacts of Large Asteroids and Comets on the Earth: Geological Society of America Special Paper 190, p. 329–352.

Spero, H.J., Bijma, J., Lea, D.W., and Bemis, B.E., 1997, Effect of seawater carbonate concentration on foraminiferal carbon and oxygen isotopes: Nature, v. 390, no. 6659, p. 497–500, doi:10.1038/37333.

Stone, R., 2004, Iceland's doomsday scenario: Science, v. 306, p. 1278–1281, doi:10.1126/science.306.5700.1278.

Stothers, R.B., 1996, Major optical depth perturbations to the stratosphere from volcanic eruptions: Pyrheliometric period, 1881–1960: Journal of Geophysical Research, v. 101, no. D2, p. 3901–3920, doi:10.1029/95JD03237.

Stüben, D., Kramar, U., Berner, Z., Leosson, M., Keller, G., Adatte, T., and Stinnesbeck, W., 2002, High resolution carbon and oxygen isotope profiles of foraminifera and the Ca-normalized Sr curve of the late Maastrichtian at Elles, Tunisia: Palaeogeography, Palaeoclimatology, Palaeoecology, v. 178, p. 321–345.

Stüben, D., Kramar, U., and Berner, Z.A., 2003, Late Maastrichtian paleoclimatic and paleoceanographic changes inferred from Sr/Ca ratio and stable isotopes: Palaeogeography, Palaeoclimatology, Palaeoecology, v. 199, p. 107–127, doi:10.1016/S0031-0182(03)00499-1.

Subbarao, K.V., Bodas, M.S., Khadri, S.F.R., and Beane, J.E., 2000, Penrose Deccan 2000 Field Excursion Guide to the Western Deccan Basalt Province, Penrose Field Guides, B: New Delhi, Geological Society of India, p. 241.

Tantawy, A.A.A., 2003, Calcareous nannofossil biostratigraphy and paleoecology of the Cretaceous–Tertiary transition in the central eastern desert of Egypt: Marine Micropaleontology, v. 47, no. 3, p. 323–356.

Thordarson, T., and Self, S., 2003, Atmospheric and environmental effects of the 1783–1784 Laki eruption: A review and reassessment: Journal of Geophysical Research, v. 108, no. D1, 4011, doi:10.1029/2001JD002042.

Tobin, T.S., Ward, P.D., Steig, E.J., Olivero, E.B., Hilburn, I.A., Mitchell, R.N., Diamond, M.R., Raub, T.D., and Kirschvink, J.L., 2012, Extinction patterns, $\delta^{18}O$ trends, and magnetostratigraphy from a southern high-latitude Cretaceous-Paleogene section: Links with Deccan volcanism: Palaeogeography, Palaeoclimatology, Palaeoecology, v. 350–352, p. 180–188, doi:10.1016/j.palaeo.2012.06.029.

Uthicke, S., Momigliano, P., and Fabricius, K.E., 2013, High risk of extinction of benthic foraminifera in this century due to ocean acidification: Scientific Reports, v. 3, doi:10.1038/srep01769.

Wilf, P., Johnson, K.R., and Huber, B.T., 2003, Correlated terrestrial and marine evidence for global climate changes before mass extinction at the Cretaceous-Paleogene boundary: Proceedings of the National Academy of Sciences of the United States of America, v. 100, no. 2, p. 599–604, doi:10.1073/pnas.0234701100.

Yu, J., and Elderfield, H., 2007, Benthic foraminiferal B/Ca ratios reflect deep water carbonate saturation state: Earth and Planetary Science Letters, v. 258, p. 73–86, doi:10.1016/j.epsl.2007.03.025.

Zeebe, R.E., 2012, History of seawater carbonate chemistry, atmospheric CO_2, and ocean acidification: Annual Review of Earth and Planetary Sciences, v. 40, p. 141–165, doi:10.1146/annurev-earth-042711-105521.

Zeebe, R.E., Zachos, J.C., Caldeira, K., and Tyrrell, T., 2008, Carbon emissions and acidification: Science, v. 321, p. 51–52, doi:10.1126/science.1159124.